⟨NuMeriQS⟩

Collaborative Research Center 1639

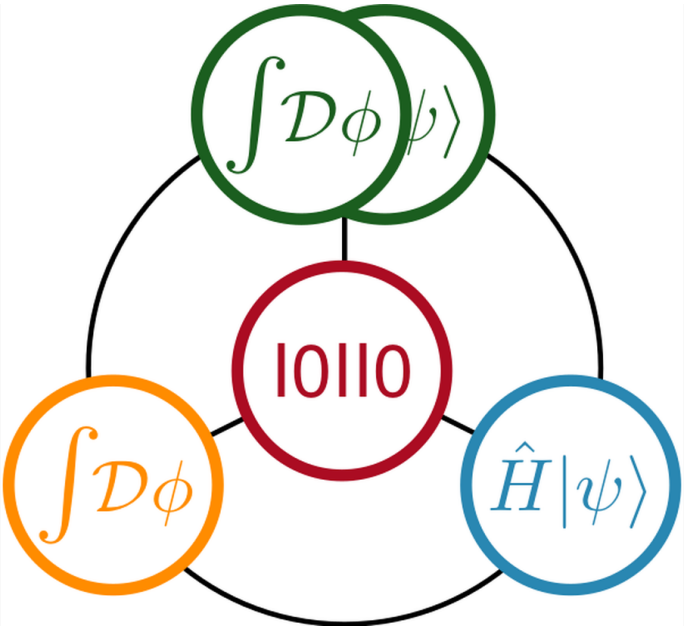

NuMeriQS Retreat 2024

Sep 30 — Oct 2 2024

Bethe Center for Theoretical Physics
University of Bonn

Book of Poster

TP A01

CRC 1639
A01
⟨NuMeriQS⟩

Modern Monte Carlo Approaches with Machine Learning Potentials for Material Science Applications

M. Griebel, B. Kirchner, C. Urbach
University of Bonn

$\hat{H}|\psi\rangle$

Summary

- Structural emergence in computational chemistry of condensed phase processes is important for understanding phase transformations in materials science.
- The formation of the **SEI** (Solid Electrolyte Interphase) in rechargeable batteries is a crucial process that affects battery performance.
- Conventional **AIMD** (Ab Initio Molecular Dynamics) methods have limitations in terms of simulation time and computational cost.
- The project aims to address these challenges by using the **HMC** (Hybrid Monte Carlo) algorithm and **ML** (Machine Learning) based force field models to efficiently simulate and analyse the high-dimensional potential energy surface associated with phase transitions and interfaces.

State of the Art

- Hybrid / Hamiltonian Monte Carlo (HMC)

$$\mathcal{H}(p,q) = \frac{1}{2}(p,p) \; - \; \ln(g(q))\,.$$

One update step of the HMC combines the following three steps:

1. Draw the conjugate momenta p from a standard normal distribution.
2. Integrate Hamilton's equations of motion

$$\dot{q} \; = \; \frac{\partial \mathcal{H}}{\partial p}, \qquad \dot{p} \; = \; -\frac{\partial \mathcal{H}}{\partial q},$$

   numerically using a symplectic integration scheme (reversible and area preserving) starting from p, q to obtain new p' and q'.
3. Accept or reject the proposal q' with probability

$$P_{\text{acc}} \; = \; \min\{1,\; \exp(-(\mathcal{H}(p',q') - \mathcal{H}(p,q))\}.$$

- Machine-Learned Interaction Potentials (various, linear and non-linear)

$$E_{ref}(\mathcal{X}) \approx E(\mathcal{X}) = \sum_{i=1}^{n} V(D_i(x_i, \mathcal{N}_i)).$$

A linear model is the **MTP** (Moment-Tensor-Potential), which is based on:

$$M_{\mu,\nu}(x_i, \mathcal{N}_i) = \sum_{x_j \in \mathcal{N}_i} f_\mu(\|r_{ij}\|; Z_i, Z_j) r_{ij}^{\otimes \nu}, \quad r_{ij}^{\otimes \nu} = \underbrace{r_{ij} \otimes \ldots \otimes r_{ij}}_{\nu \text{ times}}.$$

Methods

- Hybrid / Hamiltonian Monte Carlo Method (**M1**, **M4**)
- Machine-Learning Interaction Potentials (**M3**, **M9**, **M4**)
  - ML based ansatz: $E_{\text{ref}}(\mathcal{X}) \approx E(\mathcal{X}) = E_{\text{rep}}(\mathcal{X}) + E_{\text{ML}}(\mathcal{X}, \mathcal{Q}) + E_{\text{disp}}(\mathcal{X}) + E_{\text{elec}}(\mathcal{X})$
  - Further issues: prediction of dipole and quadrupole moments (through equivariant architectures)
- Simulation of the crystallisation process (**M7**, **M4**)

Goals

Development of new approaches and workflows to analyse and simulate long time atomistic processes of innovative functional materials for energy storage and harvesting.

- Create efficient HMC-based simulation techniques designed for phase transitions and interfaces in energy storage and harvesting materials, capable of handling reactive processes, nucleation, and melting.
- Develop ML-based force fields with high accuracy that are able to account for polarisation effects
- Validate and apply the methods in the design of materials for energy storage and harvesting, with a focus on emerging structures like SEI formation.

Preliminary Work

- Hybrid / Hamiltonian Monte Carlo (HMC)
  - Proof of concept: HMC implementation for CPU/GPU
  - Melting- and solidification curves with and without random defects

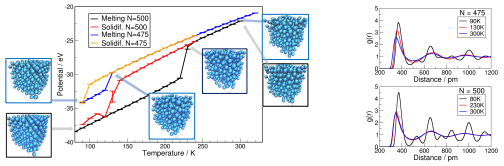

- MTP Based Machine-Learned Interaction Potentials
  - Improvement for multi-element systems
  - Training and testing error for about 4000 Ag-Pd, Cu-Pt and Ag-Pt alloys:

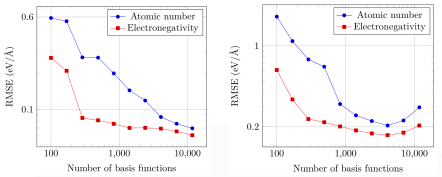

Machine learning for many-body potentials with moment tensors. T. Olbrich. Masterarbeit, Institut für Numerische Simulation, Universität Bonn, 2018.

MD vs. HMC

- Molecular Dynamics (MD) is frequently employed but has problems with rare events, as it can easily get stuck in certain configurations.
- Hybrid / Hamiltonian Monte Carlo (HMC) might be better at overcoming these energy barriers due to the frequent resampling of momenta.
- How can we quantify this?
  - MD has problems with conformational sampling of small molecules and may sample different regions of phase space based on the initial conditions.
  - Test the performance of HMC on the sampling of conformers of small molecules like Butan-2-ol.

UNIVERSITÄT BONN
⟨NuMeriQS⟩
Max-Planck-Institut für Kohlenforschung
JÜLICH Forschungszentrum

TP A02

ORCA's Automated Generator Environment For Accurate Quantum Many-Body Theory

Hang Xu, Frank Neese

Department of Molecular Theory and Spectroscopy, Max-Planck-Institut für Kohlenforschung

MAX-PLANCK-INSTITUT FÜR KOHLENFORSCHUNG

WHAT PROBLEMS ARE WE TACKLING?

- The **quantum many-body problem**, particularly the **electron correlation** problem, is of great interest in quantum chemistry and remains a significant challenge due to its highly complex nature.
- In a chemical system, the motion of electrons is never independent, leading to various interactions, including the **Coulomb interaction** from electrostatic forces and the **exchange interaction** arising from the fermionic nature of electrons. Mean-field methods like **Hartree-Fock** (**HF**) fail to capture these interactions fully, which is where post-HF methods like **Coupled Cluster** (**CC**) come into play.
- However, the process of deriving and implementing complex many-body theories like CC is remarkably demanding and requires intensive attention to detail to avoid human errors. This is where computational methods step in. **Automated code generation** has revolutionized the field by increasing robustness and efficiency, while minimizing human error during both equation derivation and code writing.
- In these automated approaches, **tensor representation** is crucial. Tensors are essential for handling the large, high-dimensional objects that arise naturally in many-body quantum mechanics. Proper utilization of **tensor contraction** tools and libraries is critical for solving such problems efficiently, enabling **large-scale calculations** in computational chemistry.
- Higher-order CC equations involve thousands of non-redundant terms, which scale poorly (e.g. O(N^7) for CCSD(T)). Meanwhile, meaningful computational work on large molecular systems requires calculations involving thousands of orbitals (**basis functions**). To manage such massive computations, **parallelization schemes** and the use of **supercomputing** resources become vital.

Define the Hamiltonian

- The non-relativistic electronic Hamiltonian under Bonn-Oppenheimer (BO) approximation:

$$\hat{H}_{\text{elec}} = \underbrace{-\sum_i^{N_e} \frac{1}{2}\nabla_i^2}_{\hat{T}_e} + \underbrace{\sum_{i,j>i}^{N_e} \frac{1}{|\mathbf{r}_i - \mathbf{r}_j|}}_{\hat{V}_{ee}} \underbrace{- \sum_i^{N_e}\sum_A^{N_N} \frac{Z_A}{|\mathbf{r}_i - \mathbf{R}_A|}}_{\hat{V}_{en}} + \underbrace{\sum_{A,B>A}^{N_N} \frac{Z_A Z_B}{|\mathbf{R}_A - \mathbf{R}_B|}}_{\hat{V}_{nn}}$$

- Rewriting using second-quantization and neglecting the nuclear-nuclear repulsion term:

$$\hat{H}_{\text{elec}} = \sum_{pq} h_{pq} \hat{a}_p^\dagger \hat{a}_q + \frac{1}{2}\sum_{p,q,r,s} \langle pq|rs\rangle \hat{a}_p^\dagger \hat{a}_q^\dagger \hat{a}_s \hat{a}_r$$

with the following definitions of electronic integrals:

$$h_{pq} = \langle p|\hat{h}|q\rangle = \int \phi_p^*(\mathbf{r}) \left(-\frac{1}{2}\nabla^2 - \sum_A^{N_N} \frac{Z_A}{|\mathbf{r} - \mathbf{R}_A|}\right) \phi_q(\mathbf{r}) d\mathbf{r}$$

$$\langle pq|rs\rangle = \iint \frac{\phi_p^*(\mathbf{r}_1)\phi_q^*(\mathbf{r}_2)\phi_r(\mathbf{r}_1)\phi_s(\mathbf{r}_2)}{|\mathbf{r}_1 - \mathbf{r}_2|} d\mathbf{r}_1 d\mathbf{r}_2$$

Define the Ansatz: Coupled Cluster

- In CC theory, the wavefunction is defined as:

$$|\Psi_{\text{CC}}\rangle = e^{\hat{T}}|\Phi_{\text{HF}}\rangle$$

in which the cluster (excitation) operators are defined as:

$$\hat{T} = \sum_m \hat{T}_m = \sum_m \frac{1}{(m!)^2} \sum_{\substack{ijk\ldots \\ abc\ldots}} t_{ijk\ldots}^{abc\ldots} \{\hat{a}_a^\dagger \hat{a}_i \hat{a}_b^\dagger \hat{a}_j \hat{a}_c^\dagger \hat{a}_k \ldots\}$$

- We can write done the Schrödinger Equation and define the **"effective"** Hamiltonian ($\bar{H}$) as:

$$\hat{H}_{\text{elec}}|\Psi_{\text{CC}}\rangle = E_{\text{CC}}|\Psi_{\text{CC}}\rangle \qquad \bar{H}|\Phi_{\text{HF}}\rangle = e^{-\hat{T}}\hat{H}_{\text{elec}}e^{\hat{T}}|\Phi_{\text{HF}}\rangle = E_{\text{CC}}|\Phi_{\text{HF}}\rangle$$

- Projecting the SE onto the ground-state and μ-body excitation manifold we obtain the energy expression together with the amplitudes equations that we need to solve:

$$E_{\text{CC}} = \langle\Phi_{\text{HF}}|\bar{H}|\Phi_{\text{HF}}\rangle = \langle\Phi_{\text{HF}}|e^{-\hat{T}}\hat{H}_{\text{elec}}e^{\hat{T}}|\Phi_{\text{HF}}\rangle \qquad \langle\Phi_\mu|\bar{H}|\Phi_{\text{HF}}\rangle = \langle\Phi_\mu|e^{-\hat{T}}\hat{H}_{\text{elec}}e^{\hat{T}}|\Phi_{\text{HF}}\rangle = 0$$

WHAT TOOLS ARE WE USING?

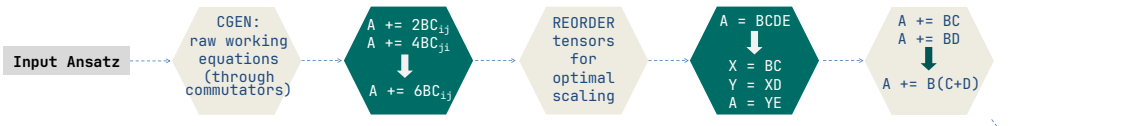

Commutator Relations and Termination Conditions

- We can re-write the effective Hamiltonian into commutator expression using the **Baker-Campbell-Hausdorff** (**BCH**) formula (truncates naturally at 4th order since the "bare" electronic Hamiltonian contains at most 2-body interaction):

$$\bar{H} = e^{-\hat{T}}\hat{H}e^{\hat{T}} = \hat{H} + [\hat{H},\hat{T}] + \frac{1}{2}[[\hat{H},\hat{T}],\hat{T}] + \frac{1}{6}[[[\hat{H},\hat{T}],\hat{T}],\hat{T}] + \frac{1}{24}[[[[\hat{H},\hat{T}],\hat{T}],\hat{T}],\hat{T}]$$

- From here, we can apply the following commutator relation to swap orders of the operators until they meet one of the termination conditions:

$$[\hat{E}_q^p, \hat{E}_s^r] = \hat{E}_s^p\delta_{rq} - \hat{E}_q^r\delta_{ps}$$

$$\hat{E}_p^i|\Phi_{\text{HF}}\rangle = 2\delta_{ip}|\Phi_{\text{HF}}\rangle \qquad \langle\Phi_{\text{HF}}|\hat{E}_i^p = 2\delta_{ip}\langle\Phi_{\text{HF}}|$$

$$\hat{E}_a^p|\Phi_{\text{HF}}\rangle = 0 \qquad \langle\Phi_{\text{HF}}|\hat{E}_p^a = 0$$

- Note here the single-particle excitation operator is defined as: $\hat{E}_q^p = \hat{a}_{p\alpha}^\dagger\hat{q}_{q\alpha} + \hat{a}_{p\beta}^\dagger\hat{q}_{q\beta}$

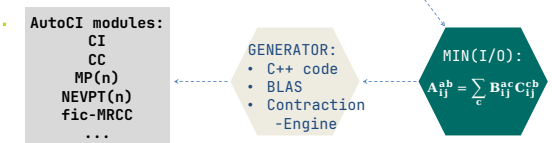

- Note on the orbital range convention:
  - p,q,r … general orbitals
  - i,j,k … occupied (inactive) orbitals
  - a,b,c … unoccupied (virtual) orbitals
  - t,u,v … active orbitals

WHAT HAVE WE ACHIEVED?

- **RHF and UHF analytic nuclear gradient**:

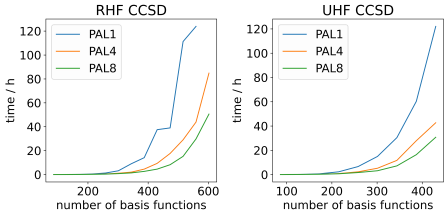

- Benchmark Settings:
  - Basis: def2-TZVP
  - Single gradient step
  - Fronzen core
  - Maxcore: 5000 MB per core
  - CPU: AMD EPYC 75F3

- **UHF analytic polarizability:**

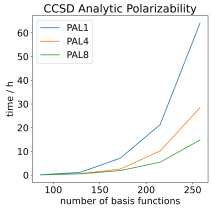

- Benchmark Settings:
  - Maxcore: 8000 MB per core
  - Basis: def2-TZVP
  - CPU: AMD EPYC 75F3
  - Unrelaxed Density

WHAT DO WE WANT NOW?

- Better performance: in equation/code generation & in generated code modules
- Better parallelization in equation/code generation & in generated code modules
- Lower scaling methods: to utilize the tensor sparsity
  - i.e. generating DLPNO code
  - requires handling of nonorthogonal basis
- (Maybe) calculation specific code generation
  - Number of virtual/occupied orbitals are provided
  - Bespoke for best performance

…

ORCA 6

(1) M. Lechner, A. Papadopoulos, K. Sivalingam, A. A. Auer, A. Koslowski, U. Becker, F. Wennmohs, F. Neese. Phys. Chem. Chem. Phys., 2024,26, 15205-15220

(2) M. Krupička, K. Sivalingam, L. Huntington, A. A. Auer, F. Neese. J. Comput. Chem. 2017, 38, 1853–1868

www.kofo.mpg.de hxu@kofo.mpg.de

TP A03

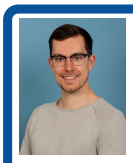


Studienstiftung des deutschen Volkes

NUMERIQS

UNIVERSITÄT BONN MCTC

A03: Uncertainty Quantification in Computational Chemistry

Tom Frömbgen[a,*], Allan Kuhn[b,*], Jürgen Dölz[b], and Barbara Kirchner[a]

[a]Mulliken Center for Theoretical Chemistry, Clausius-Institute for Physical and Theoretical Chemsitry, University of Bonn, Germany
[b]Institute for Numerical Simulation, University of Bonn, Germany
*froembgen@thch.uni-bonn.de, kuhn@ins.uni-bonn.de

Multi-level / multi-fidelity methods[1,2]

- **High-fidelity** model $f_{\text{hi}} \rightarrow$ **accurate** but **expensive**.
- **Low-fidelity** model(s) $f_{\text{lo}}^{(1)}, \ldots, f_{\text{lo}}^{(k)} \rightarrow$ **cheap** but **inaccurate**.
- **Goal**: Compute high-fidelity statistics by leveraging low-fidelity cost.

Multi-level Monte Carlo

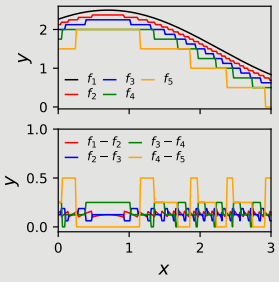

Multi-fidelity illustration

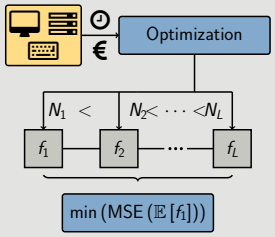

Model management strategies[1,2]

1. *Adapting*: Update low-fidelity model with high-fidelity information.
   - **Example**: Additive δ_{A} and multiplicative δ_{M} correction

$$\gamma\left(f_{\text{lo}}^{(1)} + \delta_{\text{A}}\right) + (1-\gamma) f_{\text{lo}}^{(1)} \delta_{\text{M}} = \tilde{f}_{\text{hi}} \approx f_{\text{hi}}, \ \gamma \in [0,1].$$

2. *Fusing*: Merge high-fidelity and low-fidelity models.
   - **Example**: Multi-fidelity MC estimator: $m_0 < \cdots < m_k, \alpha_i \in \mathbb{R}$

$$\mathbb{E}[f_{\text{hi}}] \approx E_{m_0}[f_{\text{hi}}] + \sum_{i=1}^{k} \alpha_i \left[E_{m_i}[f_{\text{lo}}^{(i)}] - E_{m_{i-1}}[f_{\text{lo}}^{(i)}]\right]$$

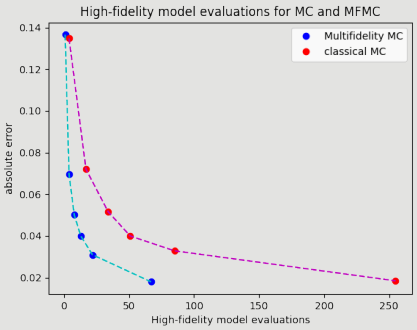

3. *Filtering*: Use high-fidelity model only when indicated by low-fidelity filter.
   - **Example**: Importance sampling: bias-density q from low-fidelity samples

$$\mathbb{P}\left(f_{\text{hi}} \in \mathcal{A}\right) \approx \sum_{i=1}^{M} 1_{f_{\text{hi}} \in \mathcal{A}}(z_i') w(z_i'), \ (z_i')_{i=1}^{M} \underset{\text{i.i.d.}}{\sim} q(z)\, dz$$

IR and VCD spectra from correlation functions[3]

$$A(\omega) \propto \int \langle \mu_i(\tau) \mu_i(t+\tau) \rangle_\tau e^{-i\omega t} dt$$

$$\Delta A(\omega) \propto \int \left[\langle \mu_i(\tau) \mathbf{m}_i(t+\tau) \rangle_\tau - \langle \mathbf{m}_i(\tau) \mu_i(t+\tau) \rangle_\tau\right] e^{-i\omega t} dt$$

$$\mu_i = \sum_j \mu_j + q_j \left(\mathbf{r}_j - \mathbf{r}_i^{\text{ref}}\right)$$

$$\mathbf{m}_i = \sum_j \left[\mathbf{m}_j + \frac{1}{2}(\mathbf{r}_j - \mathbf{r}_i^{\text{ref}}) \times \mathbf{l}_j + \frac{1}{2} q_j (\mathbf{r}_j - \mathbf{r}_i^{\text{ref}}) \times \mathbf{v}_j\right] - \frac{1}{2} \mu_i \times \mathbf{v}_i^{\text{ref}}$$

Spectra of (*R*)-butan-2-ol

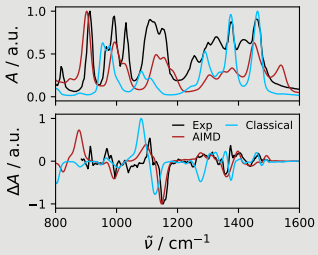

- Experiment by Wang et al.[4]
- AIMD: revPBE-D3(BJ)/DZ in CP2K
- classical spectra by neglecting atomic properties: μ_j, $\mathbf{m}_j$, $\mathbf{l}_j$

Exploring different models

Molecular dipole moments: AIMD vs. classical

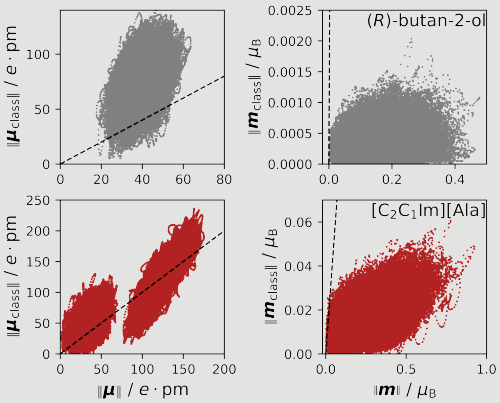

Next steps

- Determining the effect of the chemical environment on atomic properties
- Identifying suitable surrogate models for atomic and molecular properties
- Investigating machine learning models for IR and VCD spectra
- Developing a multi-fidelity UQ framework

References

[1] B. Peherstorfer, K. Willcox, M. Gunzburger, *SIAM J. Sci. Comput.* **2016**, *38*, A3163–A3194.
[2] B. Peherstorfer, K. Willcox, M. Gunzburger, *SIAM Rev.* **2018**, *60*, 550–591.
[3] M. Thomas et al., *Phys. Chem. Chem. Phys.* **2013**, *15*, 6608–6622.
[4] F. Wang, P. L. Polavarapu, *J. Phys. Chem. A* **2000**, *104*, 10683–10687.

Acknowledgements

This work was supported by the Studienstiftung des deutschen Volkes (German Academic Scholarship Foundation). This project was funded by the Deutsche Forschungsgemeinschaft (DFG, German Research Foundation) as part of the CRC 1639 NuMeriQS – project no. 511713970.

TP A04

CRC 1639 **A04** ⟨NuMeriQS⟩

Optimising the Real-Time Evolution of Quantum Spin Chains with Higher-Order Trotter Techniques

J. Ostmeyer
University of Bonn

Summary

- **Suzuki-Trotter decompositions** are important for the **time evolution of quantum systems**, splitting the time evolution operator into steps like $e^{i(A+B)t} = \left(e^{iAt/N} e^{iBt/N}\right)^N$.
- This project focuses on **quantum spin chains** (qubit systems) with the Hamiltonian $H = \sum_{i=1}^{L} \left(\sum_{a=1}^{3} J^a \sigma_i^a \sigma_{i+1}^a + h_i \sigma_i^z \right)$, but the methods are generally applicable.
- The goal of this project is to derive Trotter schemes with **reduced errors**, in particular considering their performance in practice and potential use on **quantum devices**.

State of the Art

- Suzuki's formula to construct higher order splitting methods is highly inefficient:

$$S_{n+2}(h) = S_n(s_n h)^p \, S_n\left((1-2ps_n)h\right) \, S_n(s_n h)^p \,, \qquad s_n = \frac{1}{2p - (2p)^{\frac{1}{n+1}}} \,.$$

- Feasible optimisation methods only known for two operator Hamiltonians $H = A + B$. No one-to-one correspondence to efficiencies with more operators.
- Theoretical predictions vastly overestimate errors observed in practice.
- No rigorous understanding of error accumulation over time.

Preliminary Work

Adapting 2-operator schemes for any number Λ of operators:

$$e^{(A+B)h+\mathcal{O}(h^{n+1})} = e^{Aa_1 h} e^{Bb_1 h} e^{Aa_2 h} \cdots e^{Bb_q h} e^{Aa_{q+1} h}$$

$$e^{h\sum_{k=1}^{\Lambda} A_k + \mathcal{O}(h^{n+1})} = \left(\prod_{k=1}^{\Lambda} e^{A_k c_1 h}\right)\left(\prod_{k=\Lambda}^{1} e^{A_k d_1 h}\right) \cdots \left(\prod_{k=1}^{\Lambda} e^{A_k c_q h}\right)\left(\prod_{k=\Lambda}^{1} e^{A_k d_q h}\right)$$

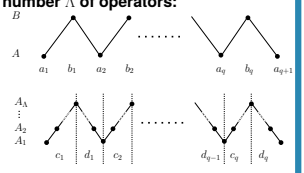

J. Ostmeyer, J. Phys. A: Math. Theor. 56, 285303 (2023)

Error accumulation:

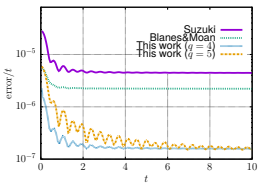

- Error scales asymptotically linear in time t.
- Precise error accumulation scheme-dependent.
- Only errors after single time step known exactly.

J. Ostmeyer, J. Phys. A: Math. Theor. 56, 285303 (2023)

Improving 4th order decompositions:

- Suzuki's method is state of the art.
- Blanes & Moan's scheme applied to $\Lambda > 2$ operators for the first time.
- New optimised schemes developed in:

J. Ostmeyer, J. Phys. A: Math. Theor. 56, 285303 (2023)

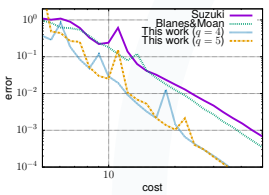

Real-time evolution:

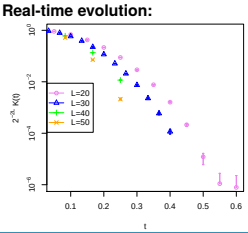

- Real-time evolution of very long quantum spin chains.
- Use reweighting and density of states techniques.
- Only short times feasible so far.

P. Buividovich and **J. Ostmeyer**, Phys. Rev. B 107, 024302 (2023)

Methods

- Tensor Network methods (primarily MPS) **(M2)** → quantum circuit optimisation
- High Performance Computing **(M4)** → high-dimensional optimisation
- Quantum Algorithms **(M5)** → real-time evolution

Approaches

- Optimise the theoretical efficiency given by the expansion

$$e^{(A+B)h+\mathcal{O}_1 h+\mathcal{O}_3 h^3+\mathcal{O}_5 h^5+\cdots} = e^{Aa_1 h} e^{Bb_1 h} \cdots e^{Bb_q h} e^{Aa_{q+1} h} \,,$$

$$\mathcal{O}_1 = (\nu-1)A + (\sigma-1)B \,, \quad \mathcal{O}_3 = \alpha[A,[A,B]] + \beta[B,[A,B]] \,, \quad \ldots$$

$$\mathrm{Eff}_2 = \frac{1}{q^2\sqrt{|\alpha|^2+|\beta|^2}} \,, \quad \ldots$$

with error coefficients $\alpha, \beta, \ldots$ defined by the chosen Trotterization.
- Perform numerical experiments with $\Lambda > 2$ operators. Identify patterns that allow to predict in practice performance for arbitrarily many operators and long times.
- Use the method by Childs et al. (PRX 11, 011020 (2021)) to predict Trotter error bounds as a baseline.

Goals

- Derive and maximise the theoretical efficiencies of order $n \geq 6$ Trotter decompositions. **Construct optimised higher order Trotter schemes** for two operators.
- Generalise **efficiency predictions** for a higher number $\Lambda > 2$ of operators and construct optimal Trotterizations in this case.
- Incorporate **in-practice** deviations from the theoretical efficiencies.
- Optimise time evolution for state-of-the-art noisy **quantum computing**.

Role within the CRC

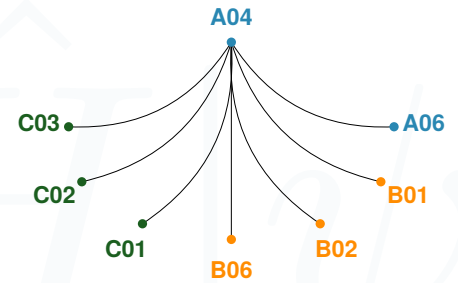

- Particularly strong connection to project **A06** treating similar physical systems and sharing an interest in optimised quantum gates for time evolution.
- Potential direct application of methods derived here in projects **C01**, **C02** & **C03**.
- Expected benefit from methods derived in projects **B01**, **B02**, **B06**.
- Important connection to project **Z02** for numerical optimisation.

UNIVERSITÄT BONN ⟨NuMeriQS⟩ Max-Planck-Institut für Kohlenforschung JÜLICH Forschungszentrum

TP A05

CRC 1639
A05
⟨NuMeriQS⟩

Integrating HPC-simulations with Data-Analysis for Structure Formation in Chemistry

B. Kirchner, P. Mutzel, E. Suarez
University of Bonn & Forschungszentrum Jülich

$\hat{H}|\psi\rangle$

Summary

- **Subject of investigation:**
  - integrated Ab Initio Molecular Dynamics (AIMD) simulations and data analysis
- **Aim: deeper understanding of molecular systems**
  - efficient use of computational resources enabling the investigation of more complex chemical problems
- **Approach:**
  - run multiple AIMD simulations simultaneously and use novel **(temporal) graph algorithms** to exchange trajectories to lead the simulation
  - develop analysis tools improving quality, efficiency, and scalability
  - utilize the **Modular Supercomputing Architecture (MSA)** to match diverse workflow requirements

State of the Art

- **AIMD simulations:** enable study of structure formation effects in complex chemical systems, and vibrational spectroscopy such as Infrared, Raman, Vibrational Circular Dichroism (VCD)
  - challenge: **optimal performance** and **scalability** on large HPC systems

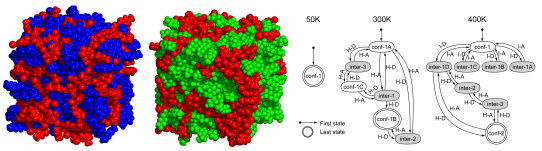

- **Graphs:** so far static structural formations and transition graphs used
  - challenge: **lack time evolution information** and **struggle to recognize similar conformations**
- **High Performance Computing:** AIMD simulations with standard parameters
  - challenge: **efficiently use heterogeneous HPC systems** by considering thread parallelism, memory management, and communication

Goals

- **AIMD:** improve capabilities and performance of AIMD simulation and **analysis** of molecular vibrational spectroscopy.
- **Graphs:** develop novel analysis methods and tools for dynamic processes based on temporal graphs
- **HPC:** improve MSA via co-design and adapt algorithms and codes to heterogeneous and modular supercomputing platforms (also see **Z02**)

Methods

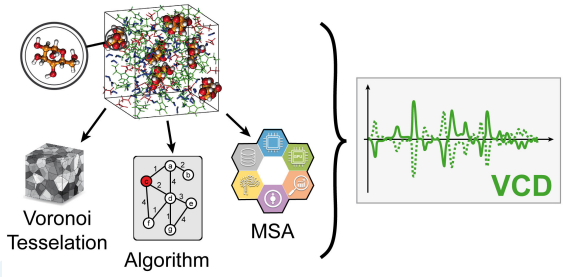

M7: Molecular Dynamics (MD)
- computational chemistry
- Ab Initio MD (AIMD)
- trajectory analysis

M9: Graph Algorithms
- temporal graph similarity
- ML using graph kernels, Graph Neural Networks (GNNs)
- graph analysis

M4: High Performance Computing & Co-design
- explore Modular Supercomputing Architecture (MSA) for large-scale simulations

Preliminary Work

AIMD:
- radical Voronoi tessellation for domain analysis and vibrational spectra calculation
- group atoms into subsets based on their local neighborhood

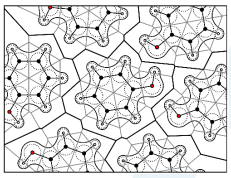

M. Brehm et int., and **B. Kirchner**, ChemPhysChem, vol. 16 (15), 2015

Temporal Graphs:

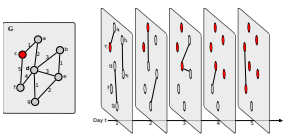

- new similarity measure for temporal graphs
- ML approach leading to improved classification rates

L. Oettershagen, et int., and **P. Mutzel**, Big Data, vol. 8 (5), 2020

MSA:
- MSA connects clusters with unique hardware configurations to meet user needs
- scaling studies on HPC systems at Jülich Supercomputing Centre (JSC)

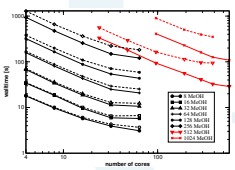

S. Taherivardanjani, et int., and **E. Suarez**, **B. Kirchner**, Advanced Theory and Simulations, vol. 5, 2021

Role within the CRC

- graph algorithms and graph learning with **A01**
- numerical methods for quantum chemistry with **A03**
- techniques of HPC and MSA optimisations with **A02** and **B02**
- generalizations of used Delaunay trinangulation with **C01**
- strong link to **Z02** for benchmarking and testing on HPC and MSA systems

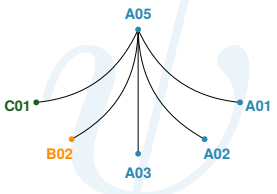

UNIVERSITÄT BONN
⟨NuMeriQS⟩
Max-Planck-Institut für Kohlenforschung
JÜLICH Forschungszentrum

TP A06

Post-measurement Quantum Monte Carlo

Using Quantum Monte Carlo to study measurement induced collective phenomenon in large many-body systems

Kriti Baweja[a,*], David J. Luitz[a], Samuel J. Garratt[b]

[a]Physikalisches Institut, University of Bonn, Germany [b]Department of Physics, University of California, Berkeley, USA

*kbaweja@uni-bonn.de

1. Background

- Key aspect of measurement is its **non-local nature** which has striking manifestation in violation of **Bell-inequality** [1].
- Measurements lead to **entanglement transition** in hybrid quantum circuits under unitary evolution [2].
- Local measurements acting on low energy states have been shown to **restructure entanglement** and **correlations** at large length scales [3].
- Theory of measured ground states and Quantum Monte Carlo (QMC) are both based on **quantum-classical mapping**.

2. Question

Can several local measurements on the ground state of highly entangled system conspire with each other to alter physical correlations?

3. Main findings

- Introducing measurement can lead to sign-problem in QMC but the focus of this work is on the sign-free scenarios.
- Singlet measurements destroy the long-range order.
- Triplet measurement enhances the long-range order.
- Correlations decay as $1/\log(x)^q$ [4], this is not known to arise in any ground state.

Singlet measurement

- Long-range singlet created with spin 1 and 7!
- Measuring singlets increases the local AFM correlations.

Unmeasured spins indicated by dash dot box

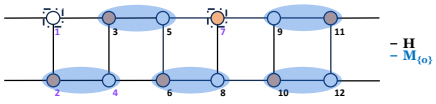

Spin-correlation along z-axis against measurement strength μ

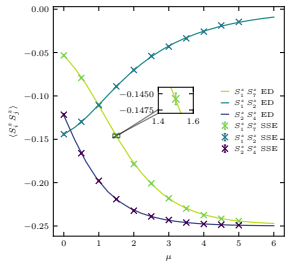

Triplet measurement

- Triplets can entangle to form total singlet.
- At $J_1/J_2 = 0.52370$ [5], the post-measurement state exhibits **surface critical behaviour**.

Measurement on diagonal bonds

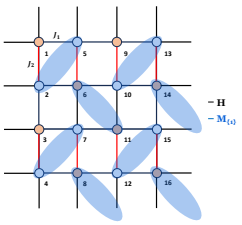

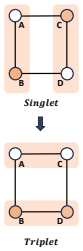

Total spin after projective measurement

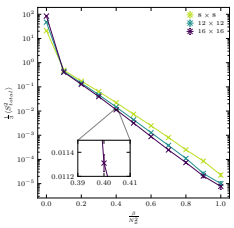

$J_1 = J_2$

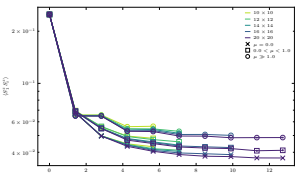

$J_1/J_2 = 0.52370$

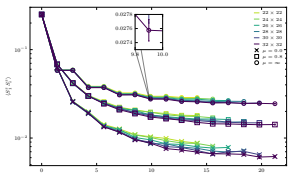

4. Method: QMC Stochastic Series Expansion

$$Z_{\{0\}}(\beta,\mu) = \mathrm{Tr}\left(e^{-\mu M_{\{0\}}} e^{-\beta H}\right)$$

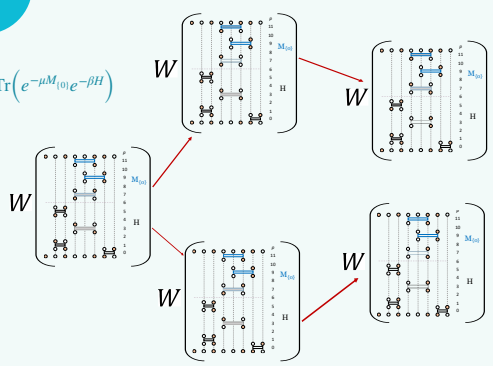

Moves in the configuration space according to the weights W of the configurations

5. Conclusion

- Measurement-induced collective phenomenon can be studied using QMC.
- Non-local aspect of the measurement process was explicitly shown with the considered systems.
- Post-measurement correlations in the critical regime of columnar dimer model exhibit *extraordinary-log* behaviour.
- Duality between measurement-induced phenomena at low energies and the statistical mechanics of critical surfaces suggests QMC as a new tool in this setting.

6. References

[1] C.H. Bennett, Phys. Rev. Lett. **70**, 1895 (1993).
[2] Y.Li, Phys. Rev. B **100**, 134306 (2019).
[3] S.J. Garratt, Phys. Rev. X **13**, 021026 (2023).
[4] M.A. Metlitski, SciPost Phys. 12,131(2022).
[5] A.W. Sandvik, AIP conference Proceedings **1297**, 135 (2010).
[6] K. Baweja, D.J. Luitz, S.J. Garratt, arXiv:2407:xxxxx.

TP B01

CRC 1639 B01 ⟨NuMeriQS⟩

An Effective Theory for Graphene Nanoribbons with Junctions

J. Ostmeyer, L. Razmadze, E. Berkowitz, T. Luu, U.-G. Meißner

Phys.Rev.B 109 (2024) 195135

Abstract

Graphene nanoribbons are a promising candidate for fault-tolerant quantum electronics. In this scenario, qubits are realised by localized states that can emerge on junctions in hybrid ribbons formed by two armchair nanoribbons of different widths. We derive an effective theory based on a tight-binding ansatz for the description of hybrid nanoribbons and use it to make accurate predictions of the energy gap and nature of the localization in various hybrid nanoribbon geometries. We use quantum Monte Carlo simulations to demonstrate that the effective theory remains applicable in the presence of Hubbard interactions. We discover, in addition to the well known localizations on junctions, which we call 'Fuji', a new type of 'Kilimanjaro' localization smeared out over a segment of the hybrid ribbon. We show that Fuji localizations in hybrids of width N and N+2 armchair nanoribbons occur around symmetric junctions if and only if $N \equiv 1 \mod 3$, while edge-aligned junctions never support strong localization. This behaviour cannot be explained relying purely on the topological Z_2 invariant, which has been believed the origin of the localizations to date.

Systems of interest

- Armchair graphene nanoribbons (AGNRs) with different widths:

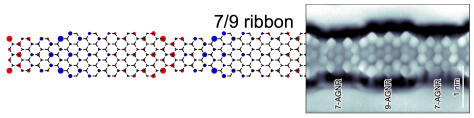

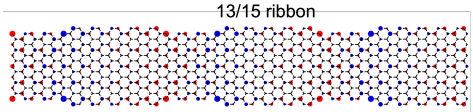

- Such systems can be experimentally engineered, see **Rizzo, D.J., Veber, G., Cao, T. et al., Nature 560, 204–208 (2018)**

Junction localization

- **Cao et al., Phys. Rev. Lett. 119, 076401 (2017)** predicted that edge geometry and width of nanoribbons dictate topological Z_2 invariant
- Bulk-boundary correspondence then leads to localization between unequal invariant systems
- Localized states correspond to lowest unfilled eigenstate

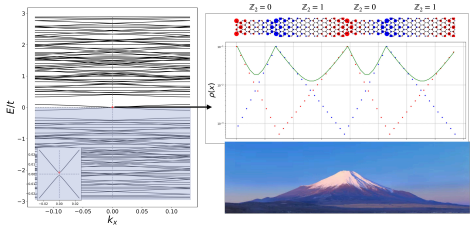

- These localizations, dubbed 'Fuji', have exp. decays on either side of the junction
- However, width of ribbon segments control decay of wavefunction: exp. vs pol.
- $\implies$ Z_2 invariance is not enough to describe such localizations

AND these results are in the non-interacting limit

Turning on interactions

- Interactions modelled by Hubbard onsite interaction U

$$\hat{H} = -t \sum_{\sigma,\langle i,j\rangle} c^\dagger_{i,\sigma} c_{j,\sigma} - \frac{U}{2} \sum_i \rho^2_{i,-} \quad ; \quad \rho_{i,-} = c^\dagger_{i,\uparrow} c_{i,\uparrow} - c^\dagger_{i,\downarrow} c_{i,\downarrow}$$

- **Monte Carlo** simulations performed in the non-perturbative regime
- Found that localizations persist in the presence of interactions, see **Luu, Meißner, Razmadze, Phys.Rev.B 106 (2022) 195422**

An Effective Theory Description of Junction Localization

- We have necessary ingredients for making an effective theory
  - Separation of scales: energy gap between lowest unfilled state to next excited state
  - Identification of low-energy degrees of freedom: localized states
  - Interactions constrained by symmetries: particle/hole (charge conjugation), sublattice ('chiral'), and time-reversal (and others)
- Can formulate 1-D ET with asymmetric hopping terms t_A and t_B
- t_A and t_B are low-energy constants (LECs) tuned to underlying *free* theory

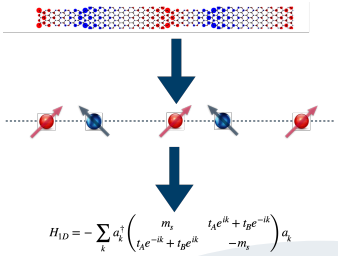

$$H_{1D} = -\sum_k a^\dagger_k \begin{pmatrix} m_s & t_A e^{ik} + t_B e^{-ik} \\ t_A e^{-ik} + t_B e^{ik} & -m_s \end{pmatrix} a_k$$

- Staggered mass m_s is LEC capturing interactions

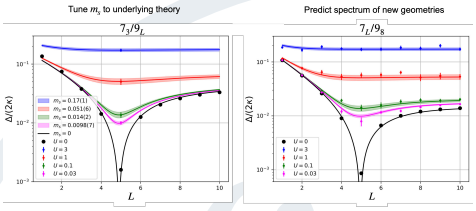

A New Type of Localization

- Found certain junctions have exponential decay on one side and power-law on the other

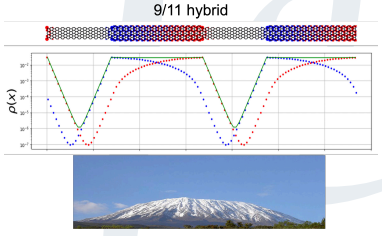

- These localizations, dubbed 'Kilimanjaro', have electrons confined between junctions

The extent of Kilimanjaro localizations can be made arbitrarily wide

UNIVERSITÄT BONN ⟨NuMeriQS⟩ Max-Planck-Institut für Kohlenforschung JÜLICH Forschungszentrum

TP B02

CRC 1639 B02 ⟨NumeriQS⟩

Towards Lattice Field Theory at the Exascale Frontier

B. Kostrzewa, S. Krieg, E. Suarez
University of Bonn & Forschungszentrum Jülich

Summary

Numerical simulations in **Lattice Field Theory (LFT)** require highly efficient algorithms capable of scaling out to very large numbers of compute nodes. Both the complexity of the simulations themselves and the rapidly evolving hardware landscape are posing unprecedented **performance-portability**, **scalability**, **maintainability** and **programmer productivity** challenges.

Project **B02** aims to develop an open-source software framework tackling these challenges, enabling future complex workflows of LFT simulations to run efficiently on heterogeneous High-Performance Computing systems based on the **Modular Supercomputing Architecture (MSA)** and to explore the integration of sampling algorithms accelerated using machine learning approaches and scalable algorithms.

State of the Art

- **domain-specific** monolithic **data-parallel** libraries for **LFT**
- frameworks interfacing with some of these libraries aiming at **programmer productivity**
- general-purpose frameworks and language extensions for **performance-portability**
- general-purpose frameworks for **task parallelism**
- the **MSA** as an approach to **exascale supercomputing**

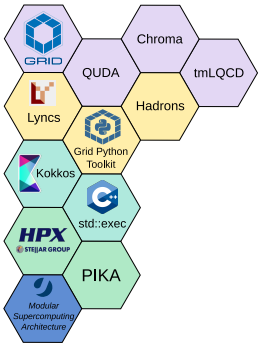

None of these currently combine **performance-portability**, **productivity**, **task parallelism** and the ability to run on the **MSA** using multiple modules (multiple architectures) at the same time.

Goals

Extend existing libraries or combine general-purpose solutions to develop a framework for lattice field theory which:

- offers domain-specific data structures, interfaces and algorithms,
- can be used from within a high-productivity language such as Python,
- is performance-portable and supports multiple simultaneous execution and memory spaces,
- exposes task parallelism at a domain-appropriate level of granularity,
- runs natively on the MSA in multi-module mode,
- implements automatic workflow generation and optimisation for complex observables.

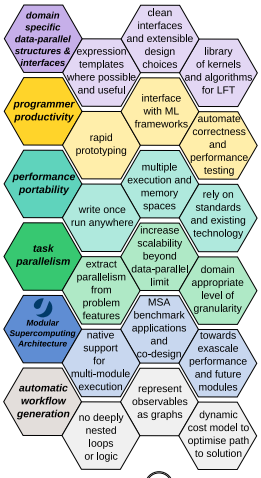

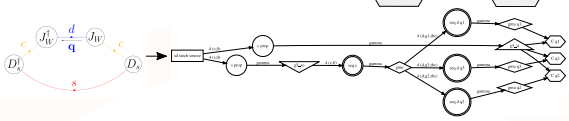

Schematic of the representation of a four-point-function as a workflow diagram with hidden and explicit parallelism suitable for a task-based approach.

Preliminary Work

Modular Supercomputing Architecture (MSA):

- Heterogeneous computer design to serve diverse user requirements

E. Suarez *et al.*, CRC Press (2019)

Twisted mass ensemble generation on GPU machines:

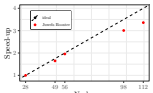

- ported 20-year-old legacy lattice quantum chromodynamics code to GPUs by extending NVIDIA QUDA library
- good scalability and performance but unsustainable → need new approach!

B. Kostrzewa, et int., *C. Urbach*, PoS LATTICE2022 (2023) 340

Algorithms for low dimensional systems:

- Optimized integrator
- Determinant filtering improving conditioning of linear systems
- Mixed precision solvers for preconditioned system

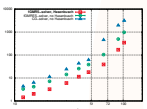

S. Krieg, *T. Luu*, *J. Ostmeyer*, P. Papaphilippou, *C. Urbach*, CPC 236, 15

Role within the CRC

- Potential direct applications in **B06**, **C01** and **A01**.
- Benefit from expertise in **A02** (automatic code generation) and in **A05** (graph algorithms).
- Exchange with **A06** on the efficient implementation of sparse matrix-vector products and with **A04** on the efficient use of the MSA.
- Exchange with **C01**, **C02** and **C03** w.r.t. simulating hitherto inaccessible parameter regions in gauge theories.
- Algorithmic overlaps with **B01** and **B05** (HMC, ML) as well as **B04** (quadrature).
- Crucial support by **Z02** in the development of systematic and reproducible benchmarking workflows and contributing to co-design efforts.

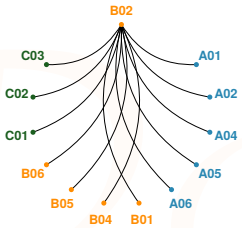

Trailblazer project for development strategies for the MSA with potential applicability in various other projects.

Methods

- **M4**: high-performance computing and co-design
- **M1**: numerical quadrature
- **M7**: molecular dynamics simulation
- **M8**: multilevel methods
- **M9**: graph algorithms and learning
- **M3**: machine learning

UNIVERSITÄT BONN ⟨NumeriQS⟩ Max-Planck-Institut für Kohlenforschung JÜLICH Forschungszentrum

TP B03

CRC 1639 B03 ⟨NuMeriQS⟩

Higher Order Quadrature for High-Dimensional Integration Problems in Lattice Field Theory

M. Griebel
University of Bonn

Summary

Predicting the average value of an observable for a lattice discretization leads to a high-dimensional integration problem. The usual approach for most lattice problems is given by Monte Carlo quadrature and Markov chain Monte Carlo sampling. There, the error is of the order $\mathcal{O}(N^{-1/2})$ with N being the number of samples. But there exist deterministic quadrature methods with higher convergence rates that may also be combined with Markov chain-type sampling. Furthermore, multilevel variants of these methods can be derived which possess further reduced cost complexities. In this project, we investigate these superior methods for lattice gauge theories.

State of the Art

- Model problems from the Kogout ladder.
- Lattice approximation: On a uniform lattice on level L for a D-dimensional field, we have the 2^{DL}-dimensional integration problem

$$I_L = \int_{\Omega_L} f_L(x_L) d\mu_L(x_L).$$

- Conventional quadrature rules suffer from the curse of dimension.
- Monte Carlo and Markov chain Monte Carlo sampling circumvent the curse but have only an accuracy of $O(N^{-1/2})$, where N is the number of used points. Moreover, they suffer from critical slowing down close to the critical temperature β^*.
- There exist higher order quadratures (QMC, Bayesian, sparse grids) which can possess an accuracy of nearly $O(N^{-r}), r > 1/2$.

Preliminary Work

- Two scales of approximation indices: In sync with the renormalization approach, approximate I_L via a restriction operator T_{L,l_1} on lattices with spacings $2^{-l_1}, l_1 = L, \ldots, 1$, i.e. by a sequence of 2^{Dl_1}-dimensional **integration problems**

$$I_{l_1} = T_{L,l_1} I_L = \int_{\Omega_{l_1}} f_{l_1}(x_{l_1}) d\mu_{l_1}(x_{l_1}), \quad l_1 = L, \ldots, 1.$$

Approximate I_{l_1} by a **quadrature method** Q_{l_1,l_2} which relates to a second index l_2. This gives for each I_{l_1} a sequence of quadrature rules

$$Q_{l_1,l_2} = \sum_{j=1}^{n_{l_2}} \alpha_{l_1,j} f_{l_1}(x_{l_1}^{(j)}), \quad l_2 \geq 1,$$

with weights $\alpha_{l_1,j} \in \mathbb{R}$ and 2^{Dl_1}-dimensional quadrature points $x_{l_1}^{(j)} \in \Omega_{l_1}$, $j = 1, \ldots, n_{l_2}$, which act on Ω_{l_1}. Here, $n_{l_2} := 2^{al_2}$ where a is a method-dependent parameter. Altogether this gives the double-indexed sequence

$$Q_{l_1,l_2} T_{L,l_1} \qquad 1 \leq l_1 \leq L, l_2 \leq 1.$$

- The **regular sparse grid combination approximation** can be written as

$$\sum_{l_1+l_2=L+1} Q_{l_1,l_2} T_{L,l_1} - \sum_{l_1+l_2=L} Q_{l_1,l_2} T_{L,l_1}.$$

It realizes a direct **multilevel** approach between lattices and quadratures and relates to a kind of bivariate extrapolation.

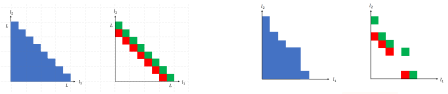

- For general index sets $\Lambda(K)$ there is the **generalized combination method**

$$\sum_{(l_1,l_2)\in\Lambda(K)} c_{l_1,l_2} Q_{l_1,l_2} T_{L,l_1} \quad \text{where} \quad c_{l_1,l_2} = \sum_{(z_1,z_2)=(0,0)}^{(1,1)} (-1)^{z_1+z_2} \chi_{\Lambda(K)}((l_1,l_2)+(z_1,z_2))$$

with characteristic function $\chi_{\Lambda(K)}$.

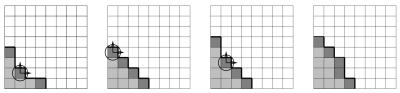

The index set $\Lambda(K)$ can be **adaptively** build up based on error indicators and cost and a benefit/cost ratio concept involving knapsack optimization.

Methods

- Quadrature techniques (**M1**): Monte Carlo, Quasi Monte Carlo, Bayesian quadrature, sparse grid quadrature.
- Markov chain variants of these basic quadrature techniques.
- Regular sparse grid combination method as multilevel approach between lattice discretization and quadrature resolution.
- Generalized sparse grid combination method.
- Adaptive combination method steered by error indicators and cost by means of a cost-benefit approach.

Goals

- Simple one-dimensional quantum mechanical test problems.
- Antiferromagnetic $O(3)$ Heissenberg and related nonlinear sigma problems that model chiral antiferromagnetic materials.
- $SU(2)$ lattice gauge theory in (1+1) and (1+2) dimensional Euclidean space-time.
- Study properties of the various basic quadrature methods, i.e. Monte Carlo, Quasi Monte Carlo, Bayesian Monte Carlo and sparse grid quadrature, within both, the conventional combination method and its adaptive variant.
- Derive necessary algorithmic parameters and details, like scaling value a for conventional approach or shape of generated index set for adaptive method.
- Derive Markov chain variants of the basic quadrature/sampling techniques and study their properties.
- Employ Markov chain variants within the combination method to obtain multilevel versions, first in an a-priori way and then in an adaptive a-posteriori way.
- Study these methods for the one-dimensional toy problems and then for the problem class of Heisenberg models and nonlinear sigma models.
- Apply the new approaches to $SU(2)$ lattice gauge theory relying on existing codes which just have to be called as subroutines with their relevant discretization parameters in the combination method.
- Study the index sets created by the adaptive version of the combination method for the temperature β getting successively closer to the critical point β^*.

Altogether, identify good sparse grid combination methods of higher order, determine optimal parameter settings, and apply them to the above lattice problems.

Role within the CRC

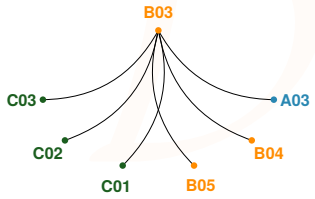

UNIVERSITÄT BONN ⟨NuMeriQS⟩ Max-Planck-Institut für Kohlenforschung JÜLICH Forschungszentrum

TP B04

CRC 1639 B04 ⟨NumeriQS⟩

Precise Perturbative Computations from Quadrature Rules

J. Dölz, C. Duhr, B. Kovačić, C. Semper
University of Bonn

Summary

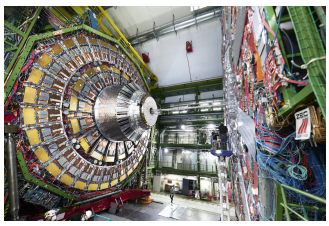

- **Motivation and state-of-the-art:** Precise perturbative predictions for collider experiments, like the Large Hadron Collider (LHC) at CERN, require the computation of complicated integrals of the 4-momenta of virtual intermediate particles.
- **Longterm goal:** Develop a numerical algorithm to evaluate Feynman integrals.
- **Goals for the first funding period:**
  1. Develop an algorithm to construct numerators rendering two-loop integrals for LHC processes finite.
  2. Develop an hp-quadrature scheme for exponential convergence, and apply it to the numerical evaluation of Feynman integrals.

State of the Art

- Amplitudes arise from often divergent Feynman integrals, with divergences cancelling each other non-trivially in the finite result
  - To control divergences, one aims to separate integrals into a finite and divergent part
  - Integrating the two parts, analytical methods are reaching their limits
  - Finite part can be integrated numerically
  - Required precision cannot be obtained using traditional Monte Carlo techniques due to slow convergence
- Integrals from boundary element methods are similar to Feynman integrals
  - Numerical treatment well understood nowadays
  - hp-approximation of kernel function using fast multipole method
  - Evaluation of singular integrals using Duffy transformations

Goals

- Split Feynman integrals into
  - Divergent part: Analytically "simple"
  - Locally finite part: Contains all the analytically complicated behaviour. Derive integrand from loop-tree duality to numerically integrate using hp-quadrature
- Develop an algorithm to generate an hp-mesh, apply hp-quadrature
- Develop publicly available software package
- Apply these numerical techniques to compute two-loop processes which are out of reach with conventional techniques, e.g., electroweak corrections processes involving vector bosons

Current Work

Integrand Analysis:

- Implemented a general algorithm to derive dual integrands from loop-tree duality
- In process: Implementation of algorithmic construction of numerator for a given Feynman integrand to obtain integrable basis for finite part

Numerical integration:

- 1D hp-interpolation theory expanded to larger class of Sobolev spaces
- Implemented hypercube based n-dimensional hp-mesh generation for integrals with singularities on co-dimension 1 hyperellipsoid

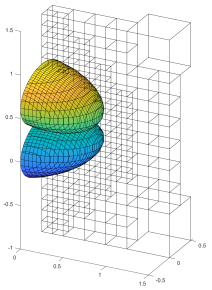

Construction of Integrands

Find a basis for the finite part of the relevant integrals
- Remove especially non-integrable IR and UV divergences
- Therefore, find algorithmic construction for most general (polynomial) numerator leading to a finite integral
- Find finite number of generators for numerator

Rewrite integrand in a form that is compatible with hp-quadrature
- Derive dual integrand from causal loop-tree duality
- Done by performing energy integration using residues

→ **Lower-dimensional finite integrals with only compact integrable singularities in the integrand**

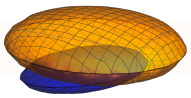

Illustration of hp-quadrature

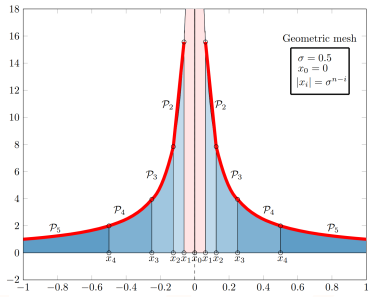

General idea of hp-quadrature:
- Partition domain of integration into subdomains with increasing size with distance to singularity
- Employ higher order quadrature rules for larger subdomains
- Regularize singular integrands using Duffy transformations

hp-interpolation in 1D:
- Using a geometric mesh, domain is subdivided such that all domain elements not bordering the singularity have p-scaling
- Elements bordering singularity have general h-scaling, which is exponential with respect to mesh size n

TP B05

CRC 1639 B05 ⟨NUMERIQS⟩

A Novel Approach to the Baryon Spectrum Based on Stochastic Methods

Ulf-G. Meißner, Deborah Rönchen
University of Bonn & IAS-4, Forschungszentrum Jülich

Summary

- Project B05 aims at extracting the light baryon resonance spectrum from experimental data and determine the uncertainties of the resonance parameters in a well-defined way. The baryon spectrum is the least understood part of the Standard Model.
- To this end, within the well-established Jülich-Bonn dynamical coupled-channel approach, we will transition from fitting with MINUIT to a Bayesian parameter estimation with the Hybrid Monte Carlo (HMC) method.

State of the Art

- Light baryon resonance spectrum: overlapping and sometimes very broad states, not visible as distinct peaks in cross section data
- Large number of inelastic channels in the medium-energy regime: extraction process even further complicated

→ Apply theoretical well-founded approaches as, e.g., **dynamical-coupled channel (DCC) frameworks**

- Numerically costly (due to the underlying theoretical complexity), large number of free model parameters
- Determination of the significance of a resonance and the parameter uncertainties: not straightforward, very challenging

→ Using a standard gradient minimization procedure (e.g. Cernlib MINUIT function minimizer) is uneconomical, if not impossible

Preliminary Work

Jülich-Bonn DCC model
purely hadronic scattering matrix:

$$T_{\mu\nu}(q,p',W) = V_{\mu\nu}(q,p',W) + \sum_\kappa \int_0^\infty dp\, p^2\, V_{\mu\kappa}(q,p,W) G_\kappa(p,W)\, T_{\kappa\nu}(p,p',W)\ ,$$

- $V_{\mu\nu}$ constructed from chiral Lagrangian
- s-channels: genuine resonance states
- t-, u-channels: background (dynamical generation of poles possible)
- 2-body unitarity and analyticity, off-shell intermediate momenta
- Resonances as poles on the 2nd Riemann sheet

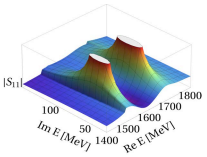

D. Rönchen, ..., U.-G. Meißner et al., Eur. Phys. J. A 49 (2013) 44

Photoproduction
in a semi-phenomenological approach:

$$\mathcal{M}_{\mu\gamma}(q,W) = V_{\mu\gamma}(q,W) + \sum_\kappa \int_0^\infty dp\, p^2\, T_{\mu\kappa}(q,p,W) G_\kappa(p,W) V_{\kappa\gamma}(p,W)\ .$$

- $V_{\mu\gamma}$ constructed with energy-dependent polynomials
- $T_{\mu\kappa}$: identical to hadronic T-matrix
  → Universal pole positions and residues

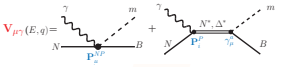

D. Rönchen, ..., U.-G. Meißner et al., Eur. Phys. J. A 50 (2014) 101

Simultaneous analysis of $\pi\mathbf{N}, \gamma\mathbf{p} \to \pi\mathbf{N}, \eta\mathbf{N}, \mathbf{K\Lambda}, \mathbf{K\Sigma}$

- 72,000 data points, ∼900 free parameters
- χ^2 minimization with MINUIT on supercomputer
- All 4-star PDG states seen, one exception: $N(1895)1/2^-$
  ↪ important for $\eta' N$ photoproduction?

D. Rönchen, M. Döring, U.-G. Meißner, Eur. Phys. J. A 58 (2022) 229

Extension to strangeness channels: in progress

- DCC framework for $\bar{K}N$ reactions → two-pole structures
- extraction of the hyperon resonance spectrum, i.e. Λ^* and Σ^* states

Methods

- Stochastic sampling: Hybrid Monte Carlo (HMC)
- Coupled-channel calculations
- Uncertainty quantification
- High-performance computing
- Effective field theories / unitarized chiral perturbation theory

Goals

- Transition from MINUIT to a Bayesian parameter estimation with HMC
- Extend the Jülich-Bonn coupled-channel model to $\gamma p \to \eta' p$
- Perform a global coupled-channel fit of pion- and photon-induced hadronic reactions

One question, e.g. : is there a $\eta' p$ cusp effect responsible for the backward peak in recent $\gamma p \to \eta p$ data?

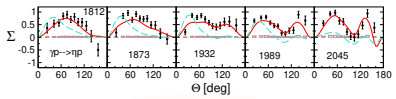

Data: CBELSA/TABS (PRL 125 (2020), 152002). Red lines: JüBo2022, dashed, cyan lines: P_{13} resonances switched off.

- Extract the resonance parameters of N^* and Δ states with well-defined uncertainties from the samples obtained with the HMC method
- In the future, this work will also be applied to strangeness baryon resonances, i.e. the spectrum of Λ^* and Σ^* states

Role within the CRC

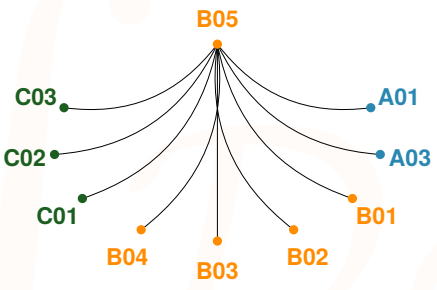

UNIVERSITÄT BONN ⟨NUMERIQS⟩ Max-Planck-Institut für Kohlenforschung JÜLICH Forschungszentrum

TP B06

CRC 1639 B06 ⟨NuMeriQS⟩

Multi-Level Iterative Solvers for Lattice Dirac Operators

S. Krieg, M. A. Schweitzer
Forschungszentrum Jülich & University of Bonn

Summary

- **Runtimes** of lattice quantum chromodynamics (LQCD) simulations remain, despite considerable algorithmic progress, **dominated** the **computational cost** associated with the **approximate solution** of the **Dirac equation**, a very large sparse linear system $Dz = b$ where $D = D(U, m)$ denotes a discretisation of the Dirac operator on a four-dimensional space-time lattice which depends on a gauge field U and a mass constant m.
- Its **iterative solution** requires the **reduction of errors in all spectral components**, which can typically only be attained at a uniform rate by so-called hierarchical or multi-level methods further accelerated by Krylov methods.
- The goal of this project is the development of **a robust efficient and highly parallel linear solver** based on novel **algebraic multigrid (AMG) / algebraic multiscale (AMS)** techniques and by the integration of **machine learning (ML)** techniques into the setup of the solver.

State of the Art

- Krylov methods used in LQCD are (flexible) GMRES, GCR, BiCGstab, etc.
- Preconditioners employed are, e.g. (often using lower floating-point precision) single-level stationary linear iterations such as Jacobi-, Gauss-Seidel- SOR-iterations, or hierarchical multi-level techniques such as geometric or AMG methods.
- Single level methods become highly inefficient as quark masses are tuned towards their physical value and as lattice volumes are increased (the former necessitating the latter)
- Successful AMG approaches for LQCD currently use a multiplicative Schwarz method as smoother, a simple geometric agglomeration strategy, and an adaptive construction of the coarse grid projection.
- The use of ML techniques in LQCD is in its infancy, but first approaches to use ML for e.g. the smoother or as a learnable preconditioner exist
- Further applications of ML techniques are based on geometric multi-grid, which is known to perform poorly for LQCD and GCNNs, which may be overkill for the highly structured LQCD

Preliminary Work

DD-α-AMG: Adaptive Aggregation Based Domain Decomposition Multigrid

- MG method for LQCD
- Wilson and TMF
- Widely adopted
- Our benchmark

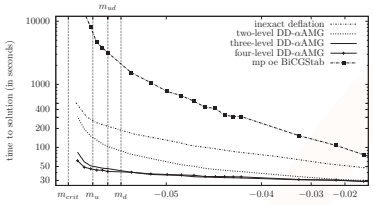

Frommer, Kahl, **Krieg**, Leder, Rottmann, SIAM J. Sci. Comput. 36 (2014) A1581-A1608

Algebraic multiscale approach and AMG

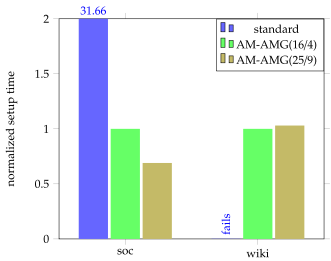

- AMS inspired coarsening and interpolation for aggregative AMG
- Improved parallelizability
- Reduced memory footprint
- Suitable for large problems

Ehrmann, Gries, **Schweitzer**, Comput Geosci 24, 683–696 (2020)

Error reduction in **all spectral components** due to multi-level structure: smoothing and coarse grid defect correction.

Methods

- Adaptive aggregative Multigrid **M8**
- Domain decomposition
- Algebraic multiscale
- Krylov subspace methods
- Machine learning techniques **M3**
- Preconditioning

Goals

- Krylov methods: Evaluation of induced dimension reduction methods as an alternative to GMRES or BiCG
- Multi-level preconditioner: Replacements of components of DD-α-AMG optimizing for large system sizes, small quark masses and the modular supercomputing architecture (MSA)
- Smoothing scheme: Investigation of the optimal parameter settings and components, evaluation of highly parallel smoothers, e.g. polynomial smoothers such as Chebyshev iteration, and ML approaches
- Coarsening scheme, interlevel transfer operators:
  - Investigation of aggregation strategies and their effect on parallel performance and communication aspects.
  - Extention of the AMS approach to LQCD, investigation of its efficiency.
  - Study of the enrichment of the coarse space in the context of adaptively improving the coarse space / interpolation.
  - Investigation of ML approaches for improved interpolation and restriction operators.

Role within the CRC

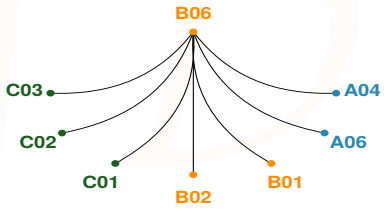

UNIVERSITÄT BONN ⟨NuMeriQS⟩ Max-Planck-Institut für Kohlenforschung JÜLICH Forschungszentrum

TP C01 – Poster 1

Using Machine Learning for Noise Resilient Optimization of Variational Quantum Eigensolvers

Luca Wagner, Kim Nicoli, Lena Funcke

Motivation — VQEs on NISQ Devices

Noisy Intermediate Scale Quantum **(NISQ)** devices may be harnessed to **outperform classical hardware** for specific optimization tasks.

Especially, hybrid quantum-classical algorithms like Variational Quantum Eigensolvers **(VQEs)** can compute **ground state energies** of quantum Hamiltonians, or complex **minimization tasks** in general.

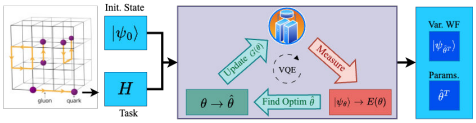

Background — VQEs and NFT Baseline

Goal:

- Find ground state and excited states of Hamiltonian H.

Quantum Device:

- Measure variational quantum circuit: get objective function $f^*(\boldsymbol{\theta}) = \langle\psi(\theta)|H|\psi(\theta)\rangle$

$|\psi(\boldsymbol{\theta})\rangle =$

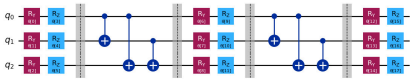

Classical Computer:

- Optimize parameters $\boldsymbol{\theta}$, given $f^*(\boldsymbol{\theta})$ – improvement by new **EMICoRe** method [1]
- Baseline method (NFT [2]) uses VQE's functional form for sequential optimization:

$$f^*(\boldsymbol{\theta}) = \boldsymbol{b}^{\mathrm{T}} \cdot \mathbf{vec}\left(\bigotimes_{d=1}^{D}\begin{pmatrix}\cos(\theta_d)\\ \sin(\theta_d)\\ 1\end{pmatrix}\right), \quad \forall \boldsymbol{\theta} \in [0, 2\pi)^D$$

- Sequential optimization of one parameter θ_d each → $f^*(\theta_d)$ becomes cosine
- Find subspace optimum: fit two equidistant measurements + previous optimum

Background — GP Regression and VQE Kernel

- Gaussian Process Regression use **Multivariate Gaussian** distribution
  - **Goal:** infer mean and variance of function values $f(\boldsymbol{\Theta}')$ from N measured noisy points $\{\boldsymbol{\Theta}, f^*(\boldsymbol{\Theta}) + \epsilon\}$, with $\boldsymbol{\Theta} = \{\boldsymbol{\theta}_1, \ldots, \boldsymbol{\theta}_N\}$.

$$p\left(\boldsymbol{f}' \mid \boldsymbol{\Theta}, \boldsymbol{y}\right) = \mathcal{N}_M\left(\boldsymbol{f}'; \boldsymbol{\mu}'_{\boldsymbol{\Theta}}, \boldsymbol{S}'_{\boldsymbol{\Theta}}\right), \quad \text{with}$$

$$\boldsymbol{\mu}'_{\boldsymbol{\Theta}} = \boldsymbol{K}'^{\top}\left(\boldsymbol{K} + \sigma^2 \boldsymbol{I}_N\right)^{-1}\boldsymbol{y}, \quad \boldsymbol{S}'_{\boldsymbol{\Theta}} = \boldsymbol{K}'' - \boldsymbol{K}'^{\top}\left(\boldsymbol{K} + \sigma^2 \boldsymbol{I}_N\right)^{-1}\boldsymbol{K}' \text{ and}$$

$$\boldsymbol{K} = k(\boldsymbol{\Theta}, \boldsymbol{\Theta}), \quad \boldsymbol{K}' = k\left(\boldsymbol{\Theta}, \boldsymbol{\Theta}'\right), \text{ and } \boldsymbol{K}'' = k\left(\boldsymbol{\Theta}', \boldsymbol{\Theta}'\right)$$

- Kernel function of the VQE can be infered from its functional form [1]:

$$k^{\mathrm{VQE}}\left(\boldsymbol{\theta}, \boldsymbol{\theta}'\right) = \sigma_0^2 \prod_{d=1}^{D}\left(\frac{\gamma^2 + \cos\left(\theta_d - \theta'_d\right)}{1 + \gamma^2}\right)$$

Method — EMICoRe's Algorithmic Procedure

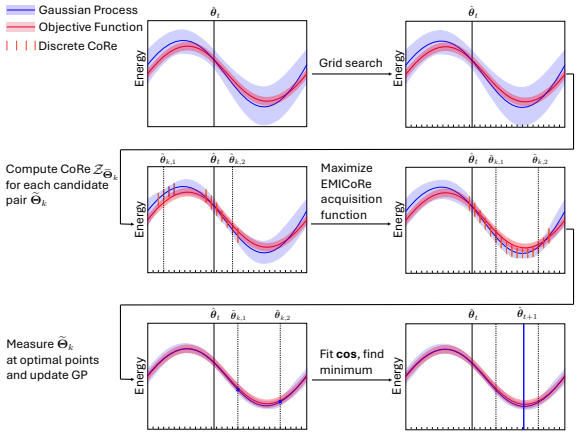

Results — Quantum Chemistry Hamiltonian

$$H = \sum_{pq} h_{pq} a_p^\dagger a_q + \frac{1}{2}\sum_{pqrs} h_{pqrs} a_p^\dagger a_q^\dagger a_r a_s$$ Adapted from [3]

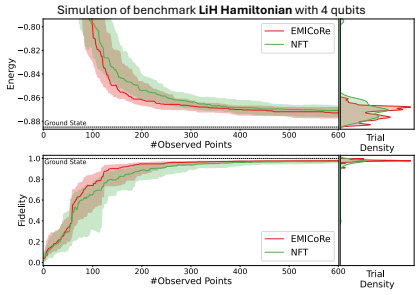

Results — Simulated Hardware Noise

$$H_{\mathrm{Ising}} = \sum_{j=1}^{Q-1}\sigma_j^X\sigma_{j+1}^X + \sum_{j=1}^{Q}\sigma_j^Z$$

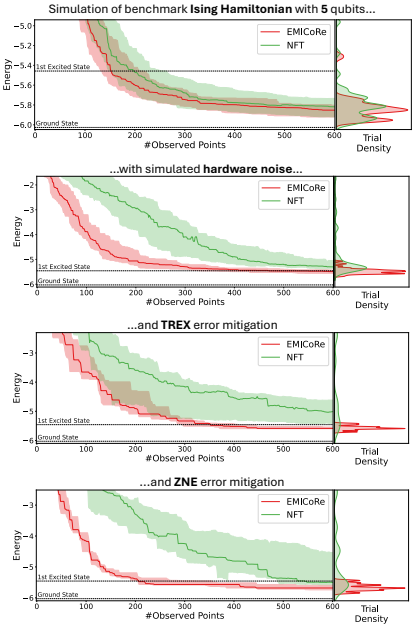

Fake5QV1() backend from **qiskit.primitives** used for noisy simulations

Conclusion

1. VQE kernel with EMICoRe acquisition function: **powerful machine-learning-based method for optimising VQEs**
2. Outperformance of state-of-the-art baseline for benchmark **Ising model**, even stronger for more complex **quantum chemistry Hamiltonian**
3. Even **stronger outperformance** when applying **simulated hardware noise**
4. Future work on application to lattice field theories, e.g. **2+1D QED**

References

[1] Nicoli, Anders, Funcke, et al. "Physics-Informed Bayesian Optimization of Variational Quantum Circuits". Proceedings of 37th Conference on Neural Information Processing Systems (NeurIPS 2023)

[2] Nakanishi, et al. "Sequential minimal optimization for quantum-classical hybrid algorithms". *Phys. Rev. Research 2, 043158* (2020)

[3] Kandala, et al. "Hardware-efficient variational quantum eigensolver for small molecules and quantum magnets". *Nature* 549, 242 (2017)

CRC 1639 C01 ⟨NuMeriQS⟩

Digitised Hamiltonian SU(2) Lattice Gauge Theories at Weak Couplings

M. Garofalo, T. Jakobs, J. Ostmeyer, C. Urbach

University of Bonn

Introduction

The Bigger Picture

- Lattice gauge theory is typically simulated in the path integral formalism. However, there is also a Hamiltonian formulation of the theory, promising easier access to real time dynamics and simulations at finite chemical potential.
- Simulations in this formalism have historically been prohibitively expensive. Recent developments in tensor network states and quantum computing promise to mitigate this and lead to a renewed interest in this formulation.

The Hilbert Space

- The Hamiltonian acts on many particle wave functions $\psi(\dots, U_{\mathbf{x},k}, \dots)$. The coordinate space of each particle is given by the gauge group SU(2). Each particle corresponds to a gauge link in connecting the sites of a cubical lattice.
- For numerical simulation the space of such wave functions needs to be discretised. This is done by first finding an appropriate set of orthogonal single particle wave functions $\hat{\phi}_n(U)$.
- A basis of the full space is then given by

$$|\dots, n_{\mathbf{x},\mathbf{k}}, \dots\rangle = \prod_{\mathbf{x},k} \hat{\phi}_{n_{\mathbf{x},\mathbf{k}}}(U_{\mathbf{x},k})\,. \tag{1}$$

Operators

Momentum Operators

The momentum operators are defined by Lie derivatives:

$$\hat{L}^c_{\mathbf{x},k}\psi = -\mathrm{i}\frac{\mathrm{d}}{\mathrm{d}\beta}\psi\left(\dots, e^{-\mathrm{i}\beta\tau_c}U_{\mathbf{x},k}, \dots\right)|_{\beta=0} \tag{2}$$

and

$$\hat{R}^c_{\mathbf{x},k}\psi = -\mathrm{i}\frac{\mathrm{d}}{\mathrm{d}\beta}\psi\left(\dots, U_{\mathbf{x},k}\,e^{\mathrm{i}\beta\tau_c}, \dots\right)|_{\beta=0}\,, \tag{3}$$

where τ_c are the generator matrices of SU(2). They are also written in a vectorized notation as

$$\hat{\vec{L}} = \sum_c \hat{L}^c_{\mu,\mathbf{x}}\tau_c \quad \text{and} \quad \hat{\vec{R}} = \sum_c \hat{R}^c_{\mu,\mathbf{x}}\tau_c\,. \tag{4}$$

Position Operators

The matrix valued position operators act as

$$\hat{U}_{\mathbf{x},k}\psi = U_{\mathbf{x},k}\,\psi(\dots, U_{\mathbf{x},k}, \dots) \tag{5}$$

and

$$\hat{U}^\dagger_{\mathbf{x},k}\psi = U^\dagger_{\mathbf{x},k}\,\psi(\dots, U_{\mathbf{x},k}, \dots)\,. \tag{6}$$

Dual Formulation

Kogut-Susskind Hamiltonian

The gauge links connect the sites of a cubical lattice:

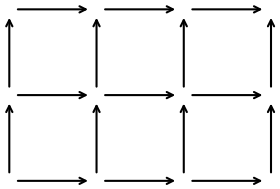

The Hamiltonian reads:

$$\hat{H}_{\mathrm{KS}} = \frac{g^2}{2}\sum_{\mathbf{x},k,c}(\hat{L}^c_{\mathbf{x},k})^2 - \frac{2}{g^2}\sum_{\mathbf{x},j<k}\mathrm{Tr}\left[\mathrm{Re}\,\hat{P}_{\mathbf{x},jk}\right] \tag{7}$$

where

$$\hat{P}_{\mathbf{x},ij} = \hat{U}_{\mathbf{x},i}\hat{U}_{\mathbf{x}+a\hat{\imath},j}\hat{U}^\dagger_{\mathbf{x}+a\hat{\jmath},i}\hat{U}^\dagger_{\mathbf{x},j}\,. \tag{8}$$

The second term, also called the magnetic term, implements an interaction between the four links of each plaquette in the lattice. When $g^2 \to 0$ this interaction dominates and makes efficient simulations of such systems quite difficult. This is why we reformulate the Hamiltonian to the dual Hamiltonian.

Dual Hamiltonian

In the Dual formulation we introduce an additional plaquette link at each site.

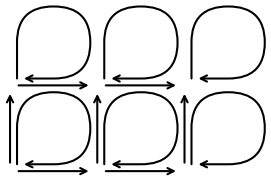

The Hamiltonian then transforms to

$$\hat{H}_{\mathrm{dual}} = g^2\sum_{\mathbf{x},k}\mathrm{Tr}\left[\left(\hat{\tilde{L}}_{\mathbf{x},k} + \tilde{\nabla}_k(U)E_{\mathbf{x}}\right)^2\right] - \frac{2}{g^2}\sum_{\mathbf{x}}\mathrm{Tr}\left[\mathrm{Re}\,\hat{U}_{\mathbf{x}}\right] \tag{9}$$

where

$$\nabla_1(U)E_{\mathbf{x}} = \hat{\tilde{R}}_{\mathbf{x}} + \hat{U}^\dagger_{2,\mathbf{x}-\hat{e}_2}\hat{\tilde{L}}_{\mathbf{x}-\hat{e}_2}\hat{U}_{2,\mathbf{x}-\hat{e}_2} \tag{10}$$

and

$$\nabla_2(U)E_{\mathbf{x}} = \hat{\tilde{L}}_{\mathbf{x}} + \hat{U}^\dagger_{1,\mathbf{x}-\hat{e}_1}\hat{\tilde{L}}_{\mathbf{x}-\hat{e}_1}\hat{U}_{1,\mathbf{x}-\hat{e}_1}\,. \tag{11}$$

Note that the magnetic term is now local, with an interacting electric term. This allows for efficient simulations at small couplings.

Discretising the Plaquette Links

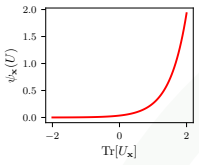

Expected shape of the single link wave function at small g^2

- First we parametrize the gauge group by spherical coordinates

$$U(\psi,\theta,\phi) = \cos(\psi)\mathbb{1} - 2\mathrm{i}\sin(\psi)\,\vec{n}(\theta,\phi)\cdot\vec{\tau} \tag{12}$$

where $\vec{n}(\theta,\phi) = (\sin\theta\cos\phi, \sin\theta\sin\phi, \cos\theta)^T$. (13)

- With this we can make an Ansatz for the basis functions:

$$B_{n,l,m} = C_n(\psi)\,Y_{l,m}(\theta,\phi) \tag{14}$$

- $C_n(\psi)$ is constructed from Hermite-Polynomials H_n as

$$C_n(\psi) \sim \frac{1}{\sin\psi}\frac{1}{\sqrt{\pi^2-\psi^2}}H_{2n+1}(u(\psi))\,\mathrm{e}^{-\frac{u^2(\psi)}{2}} \tag{15}$$

Here $u = \sqrt{\alpha}\tanh^{-1}(\psi/\pi)$ is needed to get orthogonal functions. The parameter α needs to be tuned for a given coupling. The resulting functions are well suited to approximate wave functions as the one sketched on the left.

Results

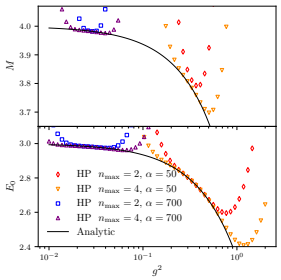

2×2 System

- On the left we show the ground state energy E_0 and mass gap $M = E_1 - E_0$ of the digitised Hamiltonian as a function of the coupling g^2.
- At a given value of α we see good agreement with the analytic expectation around an optimal g^2.
- By increasing $n_{\max}$ the range, in which the analytic prediction is matched increases

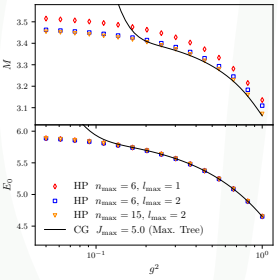

3×2 System

- Helper links are digitised using the character expansion (eigenfunctions of $\hat{\tilde{L}}^2$).
- To simulate we use matrix product states and run at optimal α for each g^2.
- The solid line shows maximum tree results, i.e. electric basis methods.
- Our method achieves good matching, and remains stable even at small couplings, where the maximum tree approach diverges.

TP C02 – Poster 1

CRC 1639 C02 ⟨NumeriQS⟩

Overcoming Ergodicity Problems of HMC using Radial Updates

F. Temmen, E. Berkowitz, A. Kennedy, T. Luu, J. Ostmeyer, X. Yu

Forschungszentrum Jülich, University of Bonn, University of Edinburgh

Summary

The sensible application of the Hybrid Monte Carlo (HMC) method to the Hubbard model is hindered by the emergence of infinite potential barriers due to a vanishing fermion determinant, resulting in an ergodicity problem that needs to be resolved. This can be achieved by augmenting the HMC algorithm with radial updates, which refer to multiplicative Metropolis-Hastings updates in a radial direction of the non-compact fields. These radial updates facilitate jumps over the potential barriers, thereby restoring ergodicity while simultaneously reducing autocorrelation times at a comparably low computational cost.

Hubbard model

The **Hubbard model** is a condensed matter model used to describe interactions of strongly-correlated electrons and consists of a nearest-neighbor tight binding term and an on-site interaction term. In the **particle-hole basis**, it is given by

$$H = -\kappa \sum_{\langle x,y \rangle} \left(a_x^\dagger a_y - b_x^\dagger b_y \right) + \frac{U}{2} \sum_x \left(a_x^\dagger a_x - b_x^\dagger b_x \right)^2, \tag{1}$$

where $(a_x, a_x^\dagger)$ and $(b_x, b_x^\dagger)$ are the ladder operators for an electron of spin-↑ and an electron-hole of spin-↓, respectively. All information about the system is then encoded in the expectation values

$$\langle \mathcal{O} \rangle = Z^{-1} \operatorname{tr}\left(\mathcal{O} e^{-\beta H} \right) \quad \text{with} \quad Z = \operatorname{tr}\left(e^{-\beta H} \right) \tag{2}$$

given in the thermal trace formalism.

Computational method

Extracting information on the Hubbard model through simulations is often achieved by utilizing the framework of **lattice field theory**, where the expectation values are given by **path integrals** over a field ϕ, such that

$$\langle \mathcal{O} \rangle = Z^{-1} \int \mathcal{D}\phi \, \mathcal{O}[\phi] e^{-S[\phi]} \quad \text{with} \quad Z = \int \mathcal{D}\phi \, e^{-S[\phi]}. \tag{3}$$

In the **importance sampling** approach, they can be approximated using an ensemble of characteristic field configurations $\{\phi^{(i)}\}_{i=1}^M$ via

$$\langle \mathcal{O} \rangle \approx \frac{1}{M} \sum_{i=1}^{M} \mathcal{O}[\phi^{(i)}], \tag{4}$$

where $\phi^{(i)} \sim e^{-S[\phi]}$. The application of this framework to the Hubbard model (1) is enabled by deriving the **Hubbard action**

$$S_H[\phi] = \frac{1}{2U\Delta_t} \sum_{t,x} \phi_{tx}^2 - \log\left(\det M[\phi|\kappa] \det M[-\phi|-\kappa] \right), \tag{5}$$

with the **fermion matrix** in the **exponential discretization** given by

$$M[\phi|\kappa]_{tx,t'y} = \delta_{t,t'}\delta_{x,y} - \left(e^{\kappa h} \right)_{xy} e^{i\phi_{tx}} \mathcal{B}_{t'} \delta_{t',t+1}. \tag{6}$$

Here, the adjacency matrix $h = \Delta_t \delta_{\langle z,z' \rangle}$, a non-compact auxiliary field ϕ and a Euclidean time dimension with lattice spacing $\Delta_t = \beta / N_t$ were introduced. The correct expectation values (3) are recovered in the continuum limit $N_t \to \infty$. Evaluating expectation values using (4) now requires generating characteristic samples $\phi \sim e^{-S_H[\phi]}$, which is subject to **Markov chain Monte Carlo** (MCMC) methods.

Hybrid Monte Carlo

The **Hybrid Monte Carlo** method [1] is a widely used MCMC algorithm that introduces a set of conjugate momenta π_{tx} to define the Hamiltonian

$$H[\phi, \pi] = \frac{1}{2} \sum_{t,x} \pi_{t,x}^2 + S[\phi]. \tag{7}$$

Using this Hamiltonian, it then constructs a Markov chain of field configurations by numerically evolving the **molecular dynamics** (MD) equations

$$\frac{d\pi}{d\tau} = -\frac{\partial H}{\partial \phi} = -\frac{\partial S}{\partial \phi} \quad \text{and} \quad \frac{d\phi}{d\tau} = \frac{\partial H}{\partial \pi} = \pi \tag{8}$$

over computer time τ along continuous trajectories in configuration space. However, the numerical evolution of (8) inevitably introduces a systematic error which can be corrected by utilizing a **Metropolis acceptance test** with

$$\alpha_{\text{HMC}} = \min\left(1, e^{-\Delta H} \right). \tag{9}$$

In general, a MCMC method is governed by a transition kernel $\Omega(\phi \to \phi')$ between subsequent configurations and it converges to a target distribution $p[\phi]$ if it is **ergodic** and satisfies the **detailed balance** condition $p[\phi]\Omega(\phi \to \phi') = p[\phi']\Omega(\phi' \to \phi)$.

Ergodicity violations in the Hubbard model

It was shown in [2] that the fermion matrix (6) vanishes on manifolds with codimension 1, giving rise to **infinite potential barriers** that separate regions in configuration space. Therefore, if the evolution of the MD equations (8) attempts to pass them, the force term $F[\phi] = -\frac{\partial S}{\partial \phi}$ diverges and the evolution is repelled. Hence, for a very fine MD integration, the HMC can not cross over into the separated regions which constitutes an **ergodicity problem** and necessitates the development of strategies for circumventing the potential barriers. [3]

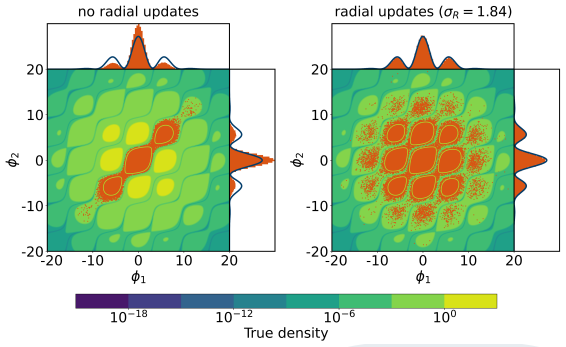

Radial updates

Radial updates are **multiplicative Metropolis-Hastings updates** of a non-compact bosonic field $\phi = (\phi_1, \ldots, \phi_d)$ that generate proposals by rescaling the **radius**

$$R = \sqrt{\sum_{i=1}^{d} \phi_i^2}. \tag{10}$$

Starting from an initial configuration ϕ, they proceed as follows:

1. **Sample an update variable** γ from a normal distribution $\mathcal{N}(\gamma | \mu = 0, \sigma_R^2)$.
2. **Rescale the radius** to generate a new configuration $\phi' = (e^\gamma \phi_1, \ldots, e^\gamma \phi_d)$.
3. Use ϕ' in a **Metropolis acceptance test** with $\alpha_R = \min\left(1, e^{-\Delta S + d\gamma}\right)$.

The radial updates are a special case of the Transformation-based MCMC algorithm [4] and satisfy the detailed balance condition. The **combination of HMC and radial updates** yields an algorithm that can efficiently jump over potential barriers and therefore **restores ergodicity**. Furthermore, radial updates **reduce autocorrelation times** at comparably **low computational cost**.

References

[1] S. Duane, A.D. Kennedy, B.J. Pendleton, and D. Roweth. *Hybrid Monte Carlo*. Phys. Lett. B, 195 (1987) 216-222

[2] M.V. Ulybyshev and S.N. Valgushev. *Path integral representation for the Hubbard model with reduced number of Lefschetz thimbles*. arXiv:1712.02188

[3] J.-L. Wynen, E. Berkowitz, C. Koerber, T.A. Lähde, and T. Luu. *Avoiding ergodicity problems in lattice discretizations of the Hubbard model*. Phys. Rev. B, 100, 075141.

[4] S. Dutta and S. Bhattacharya. *Markov chain Monte Carlo based on deterministic transformations*. Stat. Methodol. 16 (2014) 100–116

UNIVERSITÄT BONN ⟨NumeriQS⟩ JÜLICH Forschungszentrum

TP C02 – Poster 2

UNIVERSITÄT BONN · ⟨NUMERIQS⟩ · ML4Q MATTER AND LIGHT FOR QUANTUM COMPUTING

TENSOR NETWORK STUDY FOR SYMMETRY RESOLVED OTOC

Martina Gisti [1], David J. Luitz [1], Maxime Debertolis [1]

[1] *Physikalisches Institut*, University of Bonn, Germany
martina.gisti@uni-bonn.de

Abstract

The project purpose is to study the out-of-time-ordered (OTOC) in complex quantum many-body (MB) systems [1], which are usually used to investigate quantum chaos. Tensor networks (TN) are an effective technique to describe complex MB systems with low entanglement, on top of which symmetries are used to simplify further the computational complexity. This work aims to be extended to simulations of quantum MB systems on high dimensional lattices, which are challenging and physically relevant open problems. In practice, isoTNs will be implemented and extended to compute symmetry resolved OTOCs in 2D and 3D.

Tensor Network and Symmetries

- Lattice with L spins, state $|\psi\rangle \in \mathcal{H} = \mathbb{V}^{\otimes L}$ represented as a TN; in 1D matrix-product-state (MPS)

$$|\psi\rangle = \sum_{\substack{\sigma_1,\cdots,\sigma_L \\ a_0,\cdots,a_L}} M^{\sigma_1}_{a_0 a_1} M^{\sigma_2}_{a_1 a_2} \cdots M^{\sigma_L}_{a_{L-1} a_L} |\sigma_1 \cdots \sigma_L\rangle \,.$$

- Operator acting on MB system as matrix-product-operator (MPO) in 1D,

$$\hat{O} = \sum_{\sigma_1,\ldots,\sigma_L} \sum_{\sigma'_1,\ldots,\sigma'_L} \hat{O}^{\sigma_1,\sigma'_1} \ldots \hat{O}^{\sigma_L,\sigma'_L} |\sigma_1,\ldots,\sigma_L\rangle\langle\sigma'_1,\ldots,\sigma'_L|$$

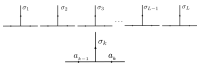

Fig. 1: MPS

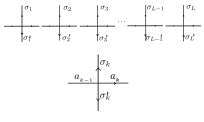

Fig. 2: MPO

Abelian Symmetry in TN

- $U(1)$: $\mathbb{V} = \bigoplus_n \mathbb{V}_n \quad \Longrightarrow \quad \hat{O} = \bigoplus_n \hat{O}_n$, block-diagonal structure of bilinear operators

$$\hat{O} = \bigoplus_n \hat{O}_n \quad \sim \quad \begin{bmatrix} (1) & 0 & \cdots & 0 \\ 0 & (2) & \cdots & 0 \\ \vdots & \vdots & \ddots & \vdots \\ 0 & 0 & \cdots & (n) \end{bmatrix}$$

- TN is $U(1)$ *symmetric* if local tensors are invariant under transformations associated to conserved quantities (*charges*), e.g. magnetization $\hat{S}^z = \sum_{j=1}^{L} \hat{S}^z_j$

$$[\hat{O}, \hat{S}^z] = 0 \qquad \Leftrightarrow \qquad \left[\hat{O}^{\sigma_j,\sigma'_j}_{a_{j-1}a_j}, \hat{S}^z\right] = 0 \quad \forall\, j$$

- Implement the $U(1)$ symmetry in TN [3]: associate to every index a *charge* q and *degeneracy* d_q, and impose the conservation of charges locally

$$\sum_{j \,\in\, \text{in}} q_j = \sum_{j \,\in\, \text{out}} q_j$$

  - physical index - spin-charge : $\sigma_j \to (n_j, d_{n_j})$
  - virtual index - flow of charges: $a_j \to (l_j - l'_j, d_{l_j - l'_j})$, $\quad l_j - l'_j = \sum_{i=1}^{j} \sigma_i - \sigma'_i$

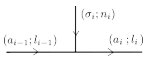

Fig. 3: MPS

MPO

- Symmetric MPO: charge conservation:

$$l_{j+1} - l'_{j+1} + n_j + n'_j = l_j - l'_j$$

- Method: consider only the non-zero elements stemming from the block-diagonal structure

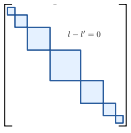

MPOs projected into symmetry sector

- **Idea:** MPO represents the projected operator into specific symmetry sector n

$$\hat{O}^{[s]} = P^{\dagger}_{[n]}\, \hat{O}\, P_{[n]}, \qquad n = \langle \hat{S}^z \rangle$$

- alternative virtual charge: $a_j \to (l_j, l'_j, d_{l_j,l'_j})$.
- computations involve smaller blocks of the matrix
- reduce the computational cost;

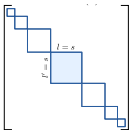

Symmetry Resolved OTOC

- Consider $\hat{S}^z_j(t) = \hat{U}(t)^{\dagger} \hat{S}^z_j \hat{U}(t)$, out-of-time-ordered correlators (OTOC), are:

$$C_{i,j}(t) = \| \, [\hat{S}^z_j(t), \hat{S}^z_i] \, \|^2_F = 1 - \frac{1}{\mathrm{Tr}\,(\mathbb{I})} \cdot \mathrm{Tr}\left(\hat{S}^z_j(t)\, \hat{S}^z_i\, \hat{S}^z_j(t)\, \hat{S}^z_i\right).$$

- **Results:** OTOCs behaviour depends on the symmetry sector n.

$$C_{i,j}(t)^{\,[n]} = 1 - \frac{1}{\mathcal{N}_n} \cdot \mathrm{Tr}\left(\left(\hat{S}^z_j(t)^{[n]}\, \hat{S}^z_i{}^{[n]}\right)^2\right), \qquad \mathcal{N}_n = \mathrm{Tr}\left(\mathbb{I}^{[n]}\right).$$

$$\mathcal{N}_n - \mathrm{Tr}(\ (S^z_b(t)^{\,n}\ \ {S^z_i}^{\,n}\ )^2\ )$$

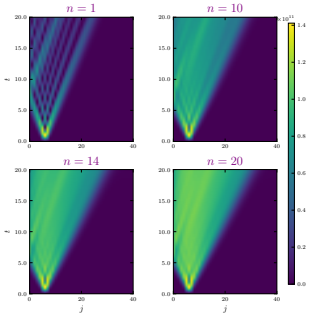

Fig. 6: OTOC in 1D system with $L = 40$ sites and isotropic Heisenberg interactions

- OTOCs have different light-cones for each sector n.

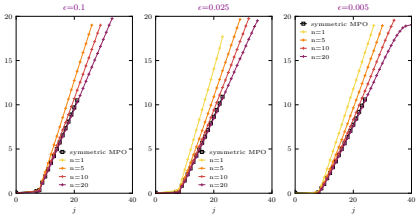

- No equipartition of the information in different symmetry sectors n.

Outlook

- DMRG with MPO in given sector
- Symmetry resolved density matrix in 1D
- OTOCs in 2D with IsoTNs, that are TNs with tailored *isometric conditions* in higher dimensions D, in order to ensure the optimal truncation [2, 4]

$$|\psi\rangle = \sum_{\substack{\sigma_1,\cdots,\sigma_L \\ a_0,\cdots,a_L}} A^{\sigma_1}_{a_0 a_1} A^{\sigma_2}_{a_1 a_2} \cdots \Psi^{\sigma_L}_{a_{L-1} a_L} |\sigma_1 \cdots \sigma_L\rangle$$

$$\sum_{\sigma_j, a_{j-1}, a_j} A^{\sigma_j}_{a_{j-1} a_j} \cdot A^{\sigma_j}_{a_{j-1} a_j}{}^{[*]} = \mathbb{I}$$

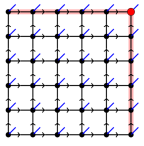

References

[1] Martina Gisti, Maxime Debertolis, and David J. Luitz. "Tensor Network Study for Symmetry Resolved OTOC". In: *arXiv:2407.xxxxx* (2024).

[2] Wilhelm Kadow, Frank Pollmann, and Michael Knap. "Isometric tensor network representations of two-dimensional thermal states". In: *Phys. Rev. B* (2023). DOI: 10.1103/PhysRevB.107.205106.

[3] Sukhwinder Singh, Robert Pfeifer, and Guifre Vidal. "Tensor network states and algorithms in the presence of a global U(1) symmetry". In: *Physical Review B* (2010).

[4] Maurits S. J. Tepaske and David J. Luitz. "Three-dimensional isometric tensor networks". In: *Phys. Rev. Res.* (2021). DOI: 10.1103/PhysRevResearch.3.023236.

TP C03

Equivariant Normalizing Flows for the Hubbard Model

Janik Kreit, D. Schuh, E. Berkowitz, L. Funcke, T. Luu, K. Nicoli, M. Rodekamp

Introduction | Hubbard Model

- Model for electron-electron interaction on lattice [1] e.g. graphene
- Fermionic Hamiltonian:

$$\mathcal{H} = \underbrace{-\kappa \sum_{\langle x,y \rangle} \left(a^\dagger_{x,\sigma} a_{y,\uparrow} + a^\dagger_{x,\sigma} a_{y,\downarrow} \right)}_{\text{hopping term}} \underbrace{- \frac{U}{2} \sum_x \left(n_{x,\uparrow} - n_{x,\downarrow} \right)^2}_{\text{on-site interaction}}$$

- Lattice size: N_s **spatial** and N_t **temporal** points
- Parameters: Hopping κ, on-site interaction U
- Integrate out fermions:

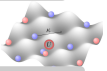

Fermion fields → Hubbard-Stratonovich transformation → Auxiliary scalar fields

- Bosonic action:

$$S = \frac{1}{2U} \sum_{x,t} \phi_{x,t}^2 - \log \det M[\phi] - \log \det M[-\phi]$$

- Parameters: Rescaled interaction strength U, fermion matrix M
- Symmetries:
  - Action: $\mathbf{Z}_2$ & **space-time translation**
  - Fermion matrix: $\mathbf{2\pi}$ **translation**

Ergodicity Problems

- **Potential barriers**: Challenging to tunnel through

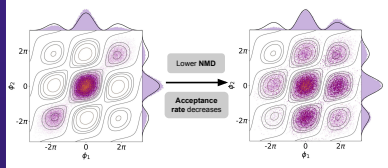

- Solid lines: Strong-coupling limit, exact for $N_s = 2$ and $N_t = 1$
- Sampler: Hamiltonian Monte Carlo (HMC)
- Ergodicity problems: Alleviated with **lower NMD**
- Downside: **Decreased acceptance rate**

Normalizing Flows[2]

- Flow from **Gaussian distribution** q_Z to **target distribution** q_0

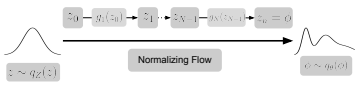

- Single layer l of **Real NVP** architecture

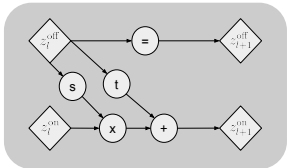

- Layer computation: alter only **on part** of z_l

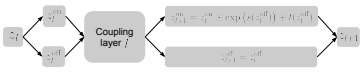

- Minimize: **KL divergence** for target distribution $p = \frac{1}{Z} e^{-S}$

$$\mathcal{L} = \mathbb{E}_{z \sim q_Z} \left[S(g_\theta(z)) - \log \left| \frac{\mathrm{d}g_\theta}{\mathrm{d}z}(z) \right| + \log q_Z(z) \right]$$

Method | Equivariant Layers

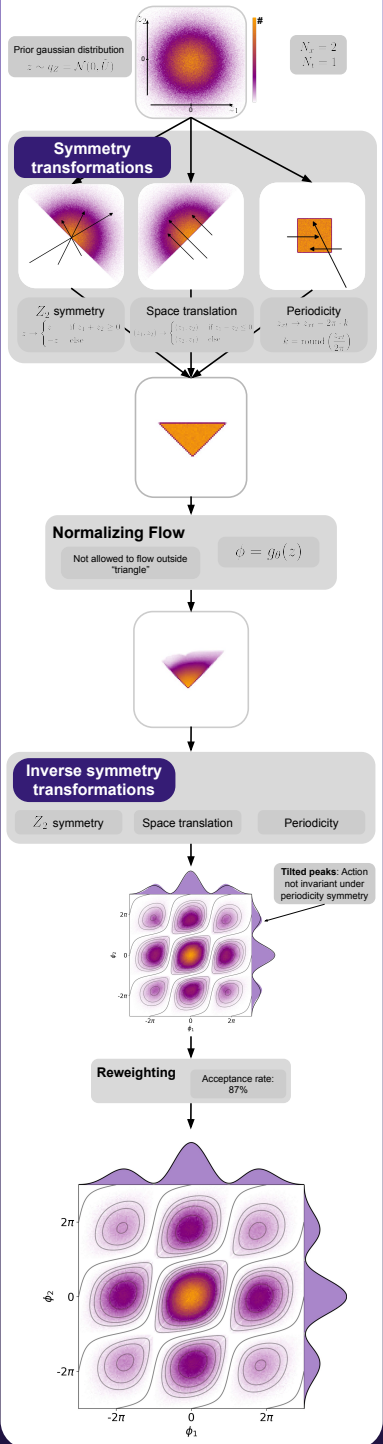

Results | Comparison

Equivariant layers **speed up** training![3]

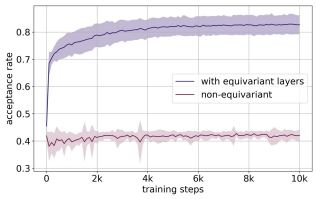

- Method:
  - 20 equivariant & 20 non-equivariant models trained
  - **Mean** and **standard deviation** of **acceptance rate** shown
- Non-equivariant: Comparable acceptance rates after 500k training steps
- Equivariant layers: Computational overhead less than 10%

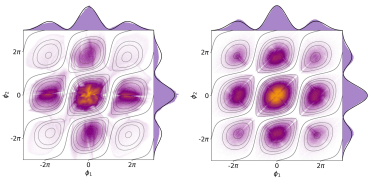

Non-equivariant
Acceptance rate: 75%
Training time: 25h

Equivariant
Acceptance rate: 85%
Training time: 16min

Summary

- **Embarrassingly parallel sampling** with normalizing flows [2]
- **First time** using normalizing flows for Hubbard Model
- **Speed up training** with equivariant layers
- **Implementation of symmetries** is advantage compared to HMC
- **High acceptance rates** across large range of hyperparameters

Outlook

- **Graphene** sized lattices [4]

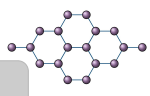

- **Honeycomb** lattices in 2+1D
- **Chemical potential**
- Various **observables**, e.g. correlators

References

[1] J. Wynen et al.,"Avoiding Ergodicity Problems in Lattice Discretizations of the Hubbard Model", PRB **100**, 075141 (2019)

[2] D. Rezende, S. Mohamed, "Variational Inference with Normalizing Flows", PMLR **37**, 1530-1538 (2015)

[3] G. Kanwar et al., "Equivariant flow-based sampling for lattice gauge theory", PRL **125**, 121601 (2020)

[4] M. Rodekamp et al., "Mitigating the Hubbard Sign Problem with Complex-Valued Neural Networks", PRB **106**, 125139 (2022)